Mechanism of inhibition of tumor angiogenesis by β-hydroxyisovalerylshikonin

Yusuke Komi,[1,2] Yasuhiro Suzuki,[1,11] Mariko Shimamura,[3,12] Sachiko Kajimoto,[4] Shigeo Nakajo,[5] Michitaka Masuda,[6] Masabumi Shibuya,[7,13] Hiroyuki Itabe,[4] Kentaro Shimokado,[2] Peter Oettgen,[8] Kazuyasu Nakaya[9] and Soichi Kojima[1,10]

[1]Molecular Ligand Biology Research Team, Chemical Genomics Research Group, Chemical Biology Department, RIKEN Advanced Science Institute, 2-1 Hiroshima, Wako, Saitama 351-0198; [2]Vascular Medicine and Geriatrics, Tokyo Medical and Dental University Graduate School, 1-5-45 Yushima, Bunkyo, Tokyo 113-8519; [3]Medical R & D Center, Tokyo Metropolitan Institute of Medical Science, 3-18-22 Honkomagome, Bunkyo, Tokyo 113-8613; [4]Laboratory of Biological Chemistry, School of Pharmaceutical Sciences, Showa University, 1-5-8 Hatanodai, Shinagawa, Tokyo 142-8555; [5]Laboratory of Biochemistry, Yokohama College of Pharmacy, 601 Minato, Totsuka, Yokohama, Kanagawa 245-0066; [6]Department of Structural Analysis, National Cardiovascular Center Research Institute, 5-7-1 Fujishirodai, Suita, Osaka 565-8565; [7]Department of Genetics, Institute of Medical Science, University of Tokyo, 4-6-1 Shirokanedai, Minato, Tokyo 108-8639, Japan; [8]Division of Cardiology, Beth Israel Deaconess Medical Center, 330 Brookline Ave., Boston, MA 02115, USA; [9]Animal Cell Biological Engineering, Niigata University of Pharmacy and Applied Life Science, Niitsu, 265-1 Higashijima, Niigata 956-8603, Japan

(Received June 30, 2008/Revised October 20, 2008/Accepted October 31, 2008)

Shikonin and β-hydroxyisovalerylshikonin (β-HIVS) from *Lithospermum erythrorhizon* inhibit angiogenesis via inhibition of vascular endothelial growth factor receptors (VEGFR) in an adenosine triphosphate-non-competitive manner, although the underlying molecular mechanism has not been fully understood. In the present study, we found that β-HIVS inhibited angiogenesis within chicken chorioallantoic membrane approximately threefold more efficiently than shikonin. β-HIVS also significantly inhibited angiogenesis in two other assays, induced either by Lewis lung carcinoma cells implanted in mouse dorsal skin or by VEGF in s.c. implanted Matrigel plugs and metastasis of Lewis lung carcinoma cells to lung. Therefore, using β-HIVS as a bioprobe, we investigated the molecular mechanism of shikonin's anti-angiogenic actions. β-HIVS inhibited the phosphorylation and expression of VEGFR2 and Tie2 without affecting VEGFR1 and fibroblast growth factor receptor 1 levels. β-HIVS suppressed the phosphorylation but not the expression of extracellular signal-regulated kinase, and an Sp1-dependent transactivation of the *VEGFR2* and *Tie2* promoters, thereby suppressing the proliferation of vascular endothelial and progenitor cells. This was mimicked by an Sp1 inhibitor mithramycin A and partially rescued by Sp1 overexpression. These results implicate potential use of shikonin and β-HIVS as leading compounds for clinical application in the future by virtue of their unique properties including: (i) inhibition of VEGFR2 and Tie2 phosphorylation in an adenosine triphosphate-non-competitive manner; (ii) simultaneous inhibition of the phosphorylation and expression of VEGFR2 and Tie2; and (iii) bifunctional inhibition of the growth in endothelial cells and vascular remodeling. (*Cancer Sci* 2009; 100: 269–277)

Angiogenesis and/or vasculogenesis are essential for the growth of solid tumors.[1] Angiogenesis is the growth and sprouting of additional blood vessels from pre-existing blood vessels, while vasculogenesis is the formation of primitive vascular networks through differentiation of vascular progenitor cells (VPC) into endothelial cells.[1] Tumor cells produce angiogenic factors, such as vascular endothelial growth factor (VEGF) and angiopoietins (Ang)-1 and -2.[2,3] The VEGF/VEGF receptor (VEGFR) signaling pathway is essential for recruiting VPC and stimulating their differentiation into endothelial cells as well as for drawing endothelial cells from pre-existing blood vessels and stimulating their growth,[1] whereas the Ang/Tie2 signaling pathway is important for sustaining interaction between endothelial and mural cells and stabilizing the vasculature.[4] VEGF and Ang-1 bind to VEGFR and Tie2, respectively, on the surface of endothelial and progenitor cells, stimulate the activities of respective receptor tyrosine kinases and exert their biological functions.

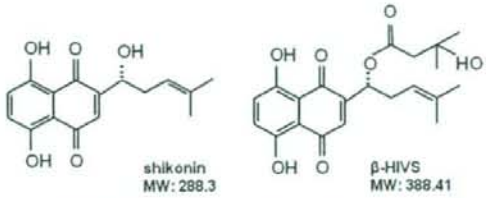

Fig. 1. Chemical structure of shikonin and β-hydroxyisovalerylshikonin (β-HIVS). MW, molecular weight.

Because newly formed blood vessels serve as a conduit for nutrition and a route for metastasis, tumor angiogenesis is a target for the treatment of solid tumors.[5] SU5416, ZD6474 and PTK787 have been developed as potent inhibitors of the phosphorylation of VEGFR tyrosine kinase.[6] A number of angiogenesis inhibitors have been developed to target receptor tyrosine kinases and/or their downstream mitogen activated protein kinase (MAPK) signaling cascades.[7]

Shikonin and β-hydroxyisovalerylshikonin (β-HIVS) are major components in the root (radix) of the plant *Lithospermum erythrorhizon*[8] (see Fig. 1 for their chemical structures), which is used traditionally as an oriental medicinal herb. They inhibit several receptor tyrosine kinases (e.g. v-Src, epidermal growth factor receptor and VEGFR) in an adenosine triphosphate (ATP)-non-competitive manner.[9] They also inhibit the growth of various lines of cancer cells and induce their apoptosis, suggesting their potential use as novel anticancer reagents.[9] Furthermore, Hisa *et al.*[10] reported that shikonin suppresses angiogenesis. However, the underlying molecular mechanism is not fully understood. Moreover, the direct effect of β-HIVS on the vascular endothelial cells and angiogenesis has not been studied.

In this manuscript, we aim to clarify the detailed molecular mechanism of anti-angiogenic activity of shikonins. First, based upon the previous report that β-HIVS inhibited tyrosine kinases

[10]To whom correspondence should be addressed.
E-mail: skojima@postman.riken.go.jp
[11]Present address: Department of Vascular Biology, Institute of Development, Aging and Cancer, Tohoku University, 4-1 Seiryo-machi, Aoba, Sendai, Miyagi 980-8575, Japan
[12]Present address: Tokyo Metropolitan Institute of Public Health, Tokyo Metropolitan Infectious Disease Surveillance Center, 3-24-1 Hyakunincho, Shinjuku, Tokyo 169-0073, Japan
[13]Present address: Department of Molecular Oncology, Tokyo Medical and Dental University Graduate School, 1-5-45 Yushima, Bunkyo, Tokyo 113-8519, Japan

doi: 10.1111/j.1349-7006.2008.01049.x

including VEGFR2 in endothelial cells stronger than shikonin, we explored the hypothesis that β-HIVS might inhibit angiogenesis stronger than shikonin and used β-HIVS to accomplish the aim. We found that β-HIVS suppressed the phosphorylation of both VEGFR2 and Tie2 as well as, surprisingly, the expression of both VEGFR2 and Tie2. This accompanied a reduction in an Sp1-dependent transactivation and upstream extracellular signal-regulated kinase (ERK) activation, culminating in reduced growth of vascular endothelial and progenitor cells, and inhibition of tumor angiogenesis. These results evidence that shikonin and β-HIVS have unique anti-angiogenic properties of bifunctional inhibition of the growth in endothelial cells and vascular remodeling and provide insights into development of novel anti-angiogenic inhibitors using shikonins as leading compounds in terms of: (i) simultaneous inhibition of the phosphorylation and expression of VEGFR2 and Tie2; and (ii) inhibition of VEGFR2 and Tie2 phosphorylation in an ATP-non-competitive manner.

Materials and Methods

Reagents. Shikonin was isolated from the plant, *Lithospermum radix*, as described before[8] and β-HIVS was purchased from Wako Pure Chemical Industries (Osaka, Japan). Mithramycin A was obtained from Sigma-Aldrich (St Louis, MO, USA). Sp1-expressing vector was constructed as described previously.[11]

Chicken chorioallantoic membrane (CAM) assay. Fertilized Dekalb chicken eggs (Omiya Kakin, Saitama, Japan) were placed in a humidified egg incubator. After a 4.5-day incubation at 38°C, a 1% solution of methylcellulose containing shikonin and β-HIVS at one of various concentrations was loaded inside a silicon ring that was placed onto the surface of the CAM. After further incubation for 2 days, a fat emulsion was injected into the chorioallantois, so that the vascular networks stood out against the white background of the lipid. Anti-angiogenic responses were evaluated under a stereomicroscope and photographed with a ×7.25 objective. Quantitative analyses were performed with angiogenesis-measuring software.[12]

Mouse dorsal air sac (DAS) assay. Millipore chambers (Millipore, Billerica, MA, USA) were filled with either RPMI-1640 medium alone or a suspension of 4×10^6 Lewis lung carcinoma (LLC) cells in the medium and sealed with membrane filters (0.45-μm pores). The chambers were implanted s.c. in DAS, created surgically by injection of an appropriate amount of air, in 7-week-old female ICR mice (Charles River, Yokohama, Japan). These mice were i.p. administered β-HIVS (30 mg/kg bodyweight) dissolved in a solution of 5% dimethylsulfoxide (DMSO), 15% Cremophor EL (Sigma-Aldrich) and 5% glucose in saline. One and three days later, the mice were killed with an overdose of diethyl ether. The skin was carefully removed and angiogenesis that had been induced around the chamber was examined under a stereomicroscope and photographed with a ×5.6 objective. Quantitative analyses were performed with angiogenesis-measuring software (ver. 2.0; KURABO, Osaka, Japan). All surgical procedures were performed under pentobarbital (Dainabot, Osaka, Japan) anesthesia. All animal experiments were performed according to the guidelines of the Animal Experiments Committee of RIKEN.

Matrigel plug assay. Matrigel (BD Biosciences, Bedford, MA, USA) was mixed with 200 units/mL heparin (Nacalai Tesque, Kyoto, Japan), with and without 50 ng/mL VEGF (Pepro Tech, Rocky Hill, NJ, USA) and 5 μM β-HIVS in 0.1% DMSO. The Matrigel mixture was injected s.c. into 5-week-old female C57BL/6 mice (Charles River). The mice were killed 7 days later. The Matrigel plugs were removed and fixed in 4% paraformaldehyde for 4 h, dehydrated through a graded ethanol series and embedded in paraffin (Nacalai Tesque). Vertical sections (5 μm) were mounted on slides and stained with hematoxylin–eosin or subjected to immunostaining as detailed below and observed under an inverted microscope (model DM IRB; Leica Microsystems, Wetzlar, Germany).

Table 1. Primers for reverse transcription polymerase chain reaction experiments

Gene		Sequence	Nucleotide#
Human *VEGFR1*	Sense	5′-TTTGGATGAGCAGTGTGAGC-3′	2415
	Antisense	5′-TTGGTTTCTTGCCTTGTTCC-3′	2866
Human *VEGFR2*	Sense	5′-GCATGGTCTTCTGTGAAGCA-3′	587
	Antisense	5′-CCAGAGATTCCATGCCACTT-3′	1018
Human *Tie2*	Sense	5′-TACACCTGCCTCATGCTCAG-3′	527
	Antisense	5′-GCAGAGACATCCTGGAAGC-3′	993
Human *FGFR1*	Sense	5′-GGCAAGGAATTCAAACCTGAC-3′	697
	Antisense	5′-CATCACGGCTGGTCTCTCTTC-3′	1224
Human *GAPDH*	Sense	5′-ACCCAGAAGACTGTGGATGG-3′	610
	Antisense	5′-CCCTGTTGCTGTAGCCAAAT-3′	1030
Human *VEGF*	Sense	5′-CTACCTCCACCATGCCAAGT-3′	48
	Antisense	5′-AAATGCTTTCTCCGCTCTGA-3′	458
Human *Ang-1*	Sense	5′-TATGCCAGAACCCAAAAAGG-3′	855
	Antisense	5′-GGGCACATTTGCACATACAG-3′	1258
Human *Ang-2*	Sense	5′-CCACAAATGGCATCTACACG-3′	878
	Antisense	5′-AAGTTGGAAGGACCACATGC-3′	1345

Metastasis assay. A suspension of 5×10^5 LLC cells was injected underneath the dorsal skin of 7-week-old female C57BL/6 mice. The mice were administered β-HIVS i.p. every other day for 3 weeks at a dose of 10 mg/kg bodyweight and killed with an overdose of diethyl ether. Lungs were carefully removed, examined under a microscope for the presence of tumors and photographed. Colonies of metastatic tumor cells observed on the whole lung surface were counted. No obvious adverse effects appeared after treatment of animals with β-HIVS under this condition.

Immunostaining. For fluorescence immunostaining, we used a combination of chicken antibodies against the cytoplasmic region of platelet/endothelial cell adhesion molecule-1 and fluorescein-5-isothiocyanate-conjugated rabbit antibodies against chicken IgG (Zymed Laboratories, Carlsbad, CA). Immunohistochemical staining of VEGFR2 was performed with an avidin–biotin kit (Vectastain Elite ABC kit; Vector Laboratories, Burlingame, CA, USA) according to the manufacturer's instructions using VEGFR2-specific rabbit monoclonal antibody (Cell Signaling Technology, Danvers, MA, USA). Immunostained sections were counterstained with Mayer's hematoxylin, dehydrated, mounted and observed under the inverted microscope.

Cell cultures. Culture of human umbilical vein endothelial cells (HUVEC) and maintenance, differentiation and sorting of the CCE/nLacZ ES cell cultures were performed as described, respectively.[12,13] VPC differentiated from CCE/nLacZ ES cell (the VEGFR2 [Flk-1] immunopositive cells) labeled with phycoerythrin were collected using the FACS VantageSE (Becton Dickinson Labware, Bedford, MA, USA) and recultured on dishes coated with type IV collagen in a modified minimum essential medium (Invitrogen, Carlsbad, CA, USA) supplemented with 10% fetal calf serum (Invitrogen). Bovine aortic endothelial cells (BAEC) were grown in a modified minimum essential medium containing 10% newborn calf serum (Hyclone Laboratories, Logan, UT, USA). NIH3T3 cells stably overexpressing VEGFR2 (NIH3T3-VEGFR2 cells) were maintained as described.[14]

Immunoprecipitation and western blotting analysis. Cells were washed several times with Tris-buffered saline (20 mM Tris-HCl, 137 mM NaCl) that contained Complete protease inhibitor cocktail (Roche, Indianapolis, IN, USA). Cells were lyzed in 1% Triton X-100 in 20 mM HEPES, pH 6.8 containing Complete protease inhibitor cocktail, 1 mM EDTA, 1 mM

doi: 10.1111/j.1349-7006.2008.01049.x

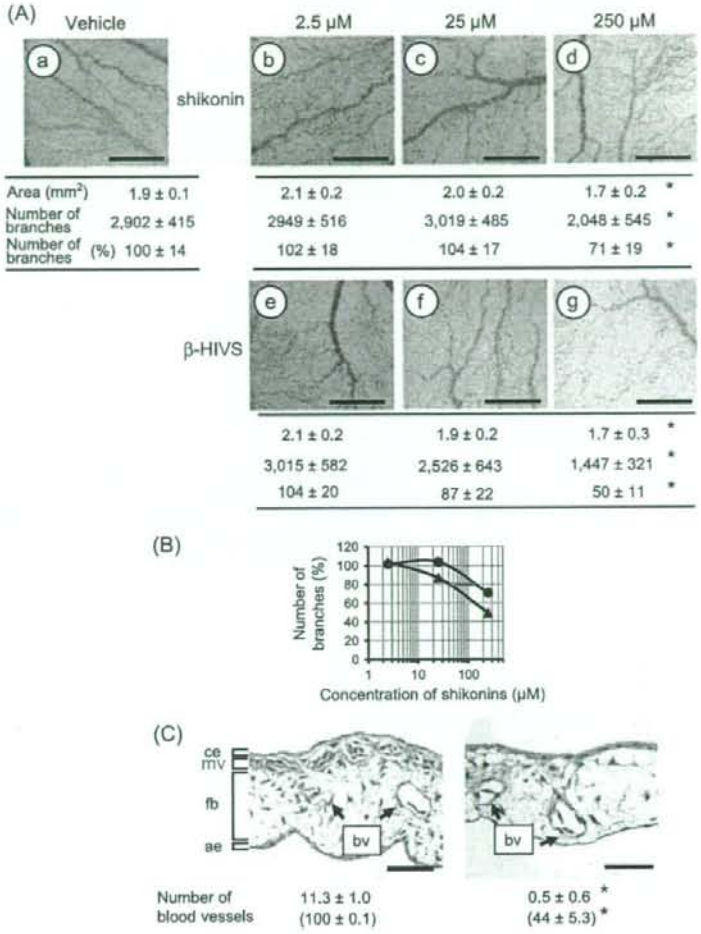

Fig. 2. Suppression of *in vivo* blood vessel formation and morphological changes induced in chicken chorioallantoic membrane (CAM) tissues by shikonins. (A) The 4.5-day-old CAM were treated with increasing concentrations of shikonin and β-hydroxyisovalerylshikonin (β-HIVS) for 48 h and then patterns of angiogenesis were photographed. (a) Vehicle (10% ethanol); (b) 2.5 μM shikonin; (c) 25 μM shikonin; (d) 250 μM shikonin; (e) 2.5 μM β-HIVS; (f) 25 μM β-HIVS; (g) 250 μM β-HIVS. Scale lines, 100 μm. The total area and the number of branches of blood vessels were analyzed with angiogenesis measuring software and are shown under each panel. Asterisks indicate significant differences ($P < 0.05$) from the control (a). A total of 18 eggs (six eggs/experiment × three experiments) were evaluated and representative results are shown. (B) Percentages of inhibition in the number of branches are plotted against concentrations of shikonin and β-HIVS. (●) Shikonin; (▲) β-HIVS. (C) The 4.5-day-old CAM were treated with vehicle (10% ethanol inside the ring = control). Note that the actual concentration of ethanol within CAM tissue was lower than that concentration due to diffusion of ethanol) (left panel) or 970 ng/egg β-HIVS (right panel) for 48 h. Vertical sections (3 μm) were mounted on slides, stained with hematoxylin–eosin, and observed under a Leica model DM IRB microscope (Leica Microsystems, Wetzlar, Germany). CAM tissue was composed of four different layers, including a thin chorionic epithelium (ce), microvasculatures (mv), a thick mesenchymal layer (fb) consisting of sparsely distributed fibroblasts and a few small blood vessels (bv), and a thin allantoic epithelium (ae). Scale lines, 50 μm. Representative micrographs from a total of 18 CAM tissues (six eggs/each × three experiments) are shown. Numbers of blood vessels were counted and are shown under each panel. Values are mean ± standard deviation ($n = 6$). Relative changes are shown as a percentage of control in parenthesis. Asterisks indicate significant differences ($P < 0.05$) from controls. (A–C) Representative results from two or three independent experiments that all gave similar results.

phenylmethylsulfonyl fluoride (PMSF) and 0.5 mM Na_3VO_5, and subjected to immunoprecipitation with anti-phosphotyrosine conjugated agarose beads (AG10; Upstate Biotechnology, Lake Placid, NY, USA) at 4°C overnight, washed with the lysis buffer three times and solubilized in sodium dodecylsulfate (SDS) buffer (200 mM Tris-HCl, pH 6.8, 6% w/v SDS, 30% glycerol, 150 mM dithiothreitol (DTT), 0.03% w/v Bromophenol Blue) followed by western analysis using Tie2-specific antibodies (1:1000 dilution, Upstate Biotechnology) or directly subjected to western analysis using phospho-VEGFR2-specific antibodies (1:1000 dilution; Cell Signaling Technology) or phospho-ERK-specific antibodies (1:2000 dilution, Cell Signaling Technology). Cell lysates were also subjected to western analysis using antibodies to VEGFR2, Tie2 and ERK, followed by reprobing with glyceraldehyde-3-phosphate dehydrogenase (GAPDH)-specific antibody (1:3000 dilution; HyTest, Turku, Finland) as a loading control. Immunoreactive bands of proteins were detected with ECL-Plus chemiluminescence reagents (GE Healthcare, Buckinghamshire, UK).

Reverse transcriptase-polymerase chain reaction (RT-PCR). Untreated (control cells) and cells treated with β-HIVS or mithramycin A were washed twice with phosphate-buffered saline and total RNA was extracted with an RNeasy Mini Kit (Qiagen, Valencia, CA, USA). RT-PCR was performed with the SuperScrip First-Strand Synthesis System (Invitrogen). Amplification by PCR was performed with pairs of specific primers summarized in Table 1.

Gel shift assay. Oligonucleotides corresponding to the GC box (Sp1 binding) motif within human VEGFR2 promoter (–85 to –64; 5′-CGGGAGAGACCCTCCTCCGCCC-3′)[15] were synthesized, double-stranded, end-labeled and used for the gel shift assays as described.[16] Nuclear proteins (6 μg) were incubated for 15 min at 4°C with 3.5 ng of ^{32}P-labeled probe in binding buffer (25 mM HEPES-KOH, 25 mM KCl, 5 mM $MgCl_2$, 50 μM $ZnSO_4$ and 8% glycerol) and separated on a 4% polyacrylamide gel at 4°C in running buffer (25 mM Tris-HCl, 190 mM glycine and 1 mM EDTA, pH 8.5). The gels were dried and radioactive bands were detected on a Fujix Bas 2500 Bio-imaging analyzer (Fuji Photo Film, Tokyo, Japan).

Transfection and luciferase assay. Transfections and assays of luciferase activity were performed as described previously[16]

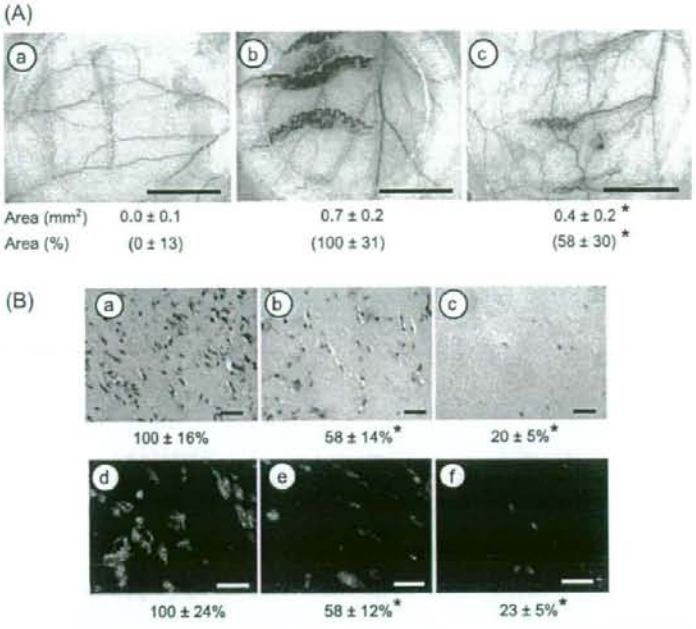

Fig. 3. Suppression of tumor-induced and vascular endothelial growth factor (VEGF)-induced *in vivo* angiogenesis by β-hydroxyisovalerylshikonin (β-HIVS) in dorsal air sac (DAS) and Matrigel plug assay. (A) DAS assay, chambers filled with either medium alone (a) or Lewis lung carcinoma (LLC) cells (b,c) were implanted into 7-week-old mice. Aliquots (100 μL) of vehicle or β-HIVS (30 mg/kg bodyweight) were injected i.p. every other day for 3 days starting at 1 day after implantation (b and c, respectively). The next day the dorsal skin was peeled off and blood vessel formation was examined under a microscope and photographed. Representative micrographs from six mice in each group are shown. Scale lines, 5 mm. Areas of tumor-induced blood vessels were analyzed with angiogenesis-measuring software and these areas are given under each photograph. Relative areas are given as percentages in parentheses. Values represent average ± standard deviation ($n = 6$). An asterisk represents a significant difference ($P < 0.05$) from the results obtained with the vehicle alone. (B) Matrigel plug assay, Matrigel plugs containing 50 ng/mL VEGF ± 5 μM or 10 μM β-HIVS were implanted into mice s.c. One week later, the Matrigel plugs were collected and stained with hematoxylin–eosin (a–c) and platelet/endothelial cell adhesion molecule-1 (PECAM-1)-specific antibody (d–f). (a,d) VEGF alone (control); (b,e) VEGF plus 5 μM β-HIVS; (c,f) VEGF plus 10 μM β-HIVS. Representative data from a total of nine micrographs (three fields × three mice) are presented. Scale lines, 100 μm. The number of invading cells in each micrograph was counted and the relative values are presented as percentages under each photograph. Values represent average ± standard error ($n = 9$, three fields × three mice). An asterisk indicates a significant difference ($P < 0.05$) from the control. (A,B) Representative results from two or three independent experiments that all gave similar results.

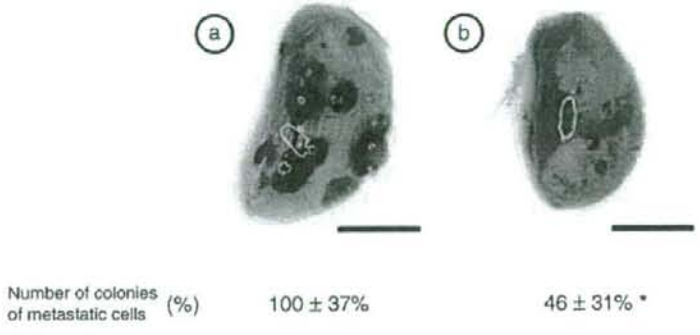

Fig. 4. Inhibition of tumor metastasis by β-hydroxyisovalerylshikonin (β-HIVS). The effect of β-HIVS on metastasis of Lewis lung carcinoma (LLC) cells was assessed as described in Materials and Methods. (a) Vehicle; (b) β-HIVS. Representative photographs from a total of five mice are shown. Relative changes in colonies of metastatic tumor cells are shown as a percentage of control in parenthesis. Scale lines, 5 mm. Values are mean ± standard deviation ($n = 5$). An asterisk indicates a significant difference ($P < 0.05$) from the control group. A representative result from two independent experiments that gave similar results is shown.

using a combination of LipofectAMINE Plus regent (Invitrogen) and a GC3-Luc vector (500 ng/dish), which was constructed by inserting a synthesized oligodeoxynucleotide cassette corresponding to three sequential repeats of the GC box motifs and TATA box upstream of the luciferase cDNA of the pGL3 vector (Promega, Madison, WI, USA), or Tie2-luc vector (500 ng/dish).[17] On the day after the transfection, the cells were washed, and treated with 5 μM β-HIVS in a medium containing 2.5% serum for 10 h, and luciferase activity of the cells was determined as before.[16]

doi: 10.1111/j.1349-7006.2008.01049.x

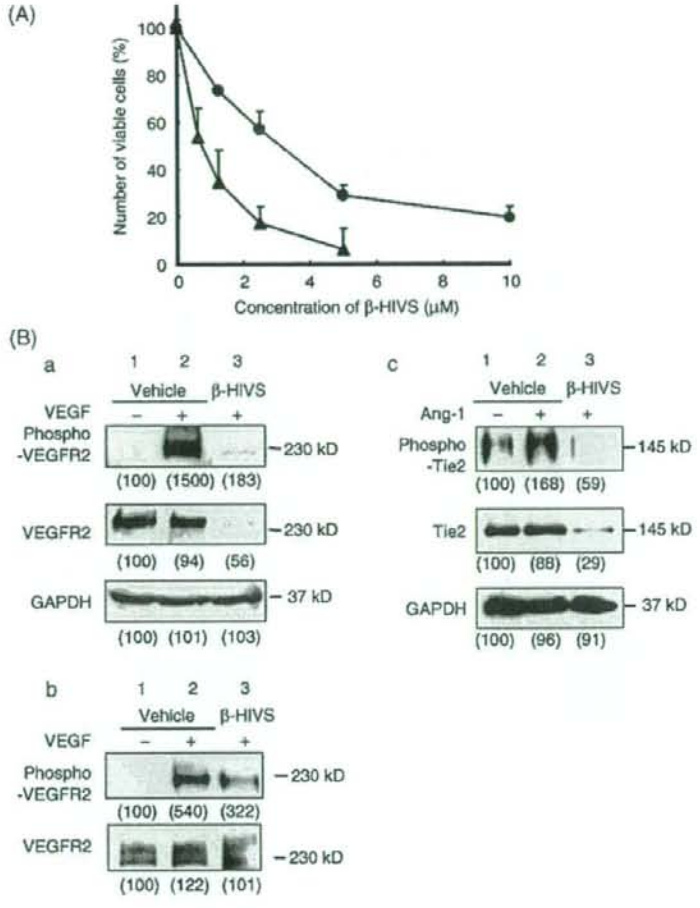

Fig. 5. Suppression by β-hydroxyisovaleryl-shikonin (β-HIVS) of vascular endothelial and progenitor cell growth accompanying reduced phosphorylation and expression of vascular endothelial growth factor receptors (VEGFR)2 and Tie2. (A) One day after human umbilical vein endothelial cells (HUVEC) or vascular progenitor cells (VPC; 1×10^5 cells) had been seeded onto 3.5-cm dishes, they were incubated for 24 h in growing medium that contained 50 ng/mL vascular endothelial growth factor (VEGF) and increasing concentrations of β-HIVS. Cells were stained with Trypan blue, and numbers of unstained viable cells were counted and plotted as percentages relative to values for untreated control cells (1.7×10^5 cells in a 3.5-cm dish). Values represent mean ± standard deviation ($n = 3$) (●) HUVEC; (▲) VPC. (B) After HUVEC and NIH-3T3-VEGFR2 cells had been incubated for 24 h with or without 5 μM β-HIVS in medium containing 2.5% serum, cells were stimulated with either 50 ng/mL VEGF (a,b), or 100 ng/mL Ang-1 (c) for 5 min, and then lyzed immediately. The amount of each phosphorylated receptor (upper panels) as well as the total amount of each receptor (middle panels) and glyceraldehyde 3-phosphate dehydrogenase (GAPDH, a loading control; lower panels) were assessed as described in Materials and Methods. (A,B) Representative results from three independent experiments that all gave similar results.

Statistical analysis. Data are expressed as mean ± standard deviation or ± standard error. Statistical significance was assessed by one-way ANOVA followed by Scheffe's Student's *t*-test.

Results

Inhibition of the blood vessel formation in CAM by β-HIVS. The effect of β-HIVS and shikonin on *in vivo* angiogenesis was examined in the CAM assay (Fig. 2A). The formation of intricate vascular networks, developing within control CAM (Fig. 2A,a), was moderately suppressed with shikonin at a concentration of 720 ng/egg (250 μM inside the ring, Fig. 2A,d), whereas β-HIVS exerted much stronger anti-angiogenic activity in a dose-dependent manner at concentrations of 9.7–970 ng/egg (corresponding to 2.5–250 μM inside the ring, Fig. 2A,e–g) (the actual concentrations of shikonin and β-HIVS within CAM tissues were lower than these concentrations due to diffusion of the drug). Treatment with 250 μM β-HIVS inhibited angiogenesis with CAM by 50%, more efficiently than 29% with 250 μM shikonin. The result of plotting the inhibition curve suggested that β-HIVS is a threefold more potent anti-angiogenic inhibitor than shikonin (Fig. 2B). Staining with hematoxylin–eosin of vertical sections of CAM tissues revealed that exposure to 250 μM β-HIVS for 48 h caused a 55% reduction in the number of capillaries that developed underneath the chorionic epithelium without affecting epithelial cells composing the chorionic membrane (Fig. 2C).

Suppression of *in vivo* angiogenesis by β-HIVS in DAS and matrigel plug assay. Figure 3A shows the result of DAS assays using murine LLC cells. From pre-existing blood vessels beneath the epidermis (Fig. 3A,a), strikingly disorganized and tortuous vessels were induced towards tumor cells in the chamber (Fig. 3A,b), which was reduced by 42% in mice administered β-HIVS at 30 mg/kg bodyweight (Fig. 3A,c). Under the same condition, the bodyweight of the mice with implanted chambers did not change significantly (data not shown). No obvious sign of toxicity in kidney vasculature and tracheal mucosa (Supplementary Fig. S1a,b) or proteinuria (Supplementary Fig. S2A) was observed in β-HIVS-administrated mice, while moderate damage was seen in the liver (Supplementary Fig. S1,f). To determine whether β-HIVS might act on blood vessel cells and inhibit blood vessel formation, we examined the effect of β-HIVS in the Matrigel plug assay (Fig. 3B). Invasion of cells was observed in the control Matrigel that contained VEGF without β-HIVS (Fig. 3B,a). When β-HIVS was administered in the Matrigel at a

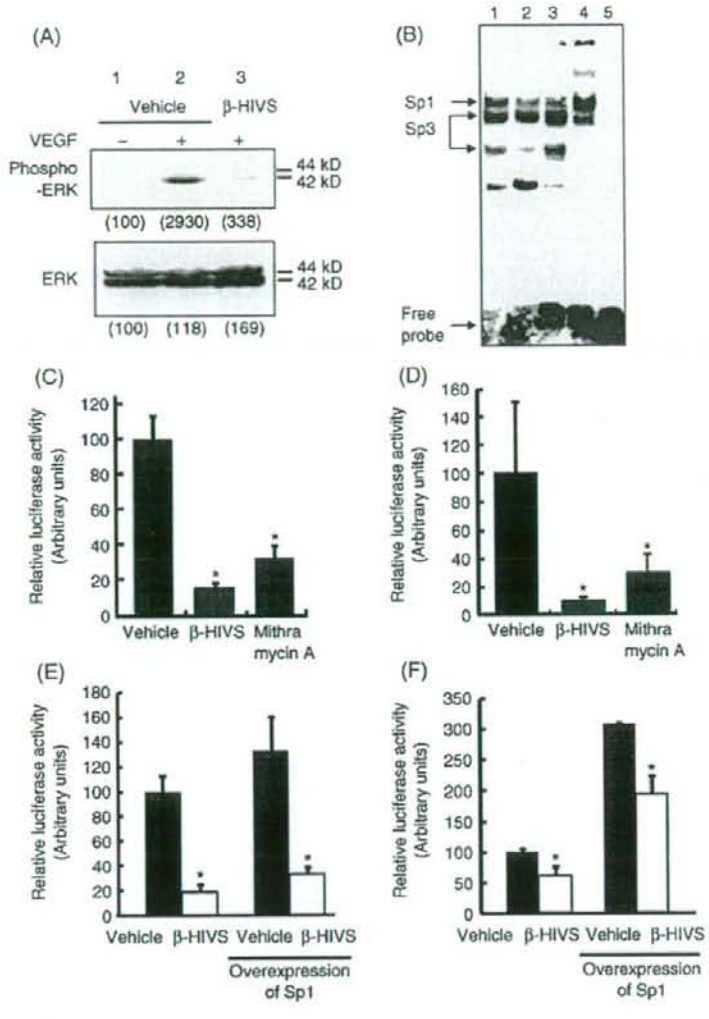

Fig. 6. Suppression in mitogen activated protein kinase (MAPK)-Sp1 pathway by β-hydroxyisovalerylshikonin (β-HIVS). (A) β-HIVS on the activation of externally regulated kinases (ERK). After human umbilical vein endothelial cells (HUVEC) had been incubated for 24 h with or without 5 μM β-HIVS in medium that contained 2.5% serum, cells were stimulated with 50 ng/mL vascular endothelial growth factor (VEGF) for 5 min, and cell lysates were prepared and subjected to western blot analysis. Upper panel, changes in phosphorylated ERK protein. Lower panel, changes in total amounts of ERK protein. (B) β-HIVS on Sp1 binding. After treatment of HUVEC with 5 μM β-HIVS for 24 h, nuclear extracts were prepared and Sp1 binding to the *VEGFR2* GC box motif was assessed by gel shift assay. Lane 1, vehicle; lane 2, 5 μM β-HIVS; lane 3, vehicle + anti-Sp1 immunoglobulin (Ig)G; lane 4, vehicle + Sp3 IgG; lane 5, vehicle + unlabeled oligonucleotide. (C) GC3 motif-luciferase reporter activity. Bovine aortic endothelial cells (BAEC) were transfected with a GC3 motif-luciferase chimeric gene construct. The day after transfection, the medium was changed and the cells were treated with 5 μM β-HIVS or 10 nM mithramycin A for 10 h. Transactivation activity was assessed by luciferase reporter assay and plotted as percentages of the values for the control (vehicle). (D) *Tie2* promoter-luciferase reporter activity. BAEC were transfected with a Tie2-luciferase chimeric gene construct. The day after transfection, the medium was changed and cells were treated with 5 μM β-HIVS or 10 nM mithramycin A for 10 h. Transactivation activity was assessed by luciferase reporter assay and plotted as percentages of the values for the control (vehicle). (E), (F) Partial rescue of β-HIVS's inhibition in GC3 motif-luciferase (E) and Tie2 promoter-luciferase (F) reporter activities with constitutively active MEK. BAECs were transfected with combinations of either a GC3 motif-luciferase (E) or a Tie2 promoter-luciferase (F) chimeric gene construct and empty vector or constitutively active MEK gene-expressing vector. The next day of transfection, medium was changed and cells were treated with 5 μM β-HIVS for 10 h. Transactivation activity was assessed as before, and plotted as percentages of the values for the control (vehicle). (A–F) Representative results from two or three independent experiments that all gave similar results. (C)–(F). Values represent means ± standard deviation ($n = 3$) Asterisks indicate significant differences ($P < 0.05$) from respective controls.

concentration of 5 μM, the VEGF-induced invasion of cells was inhibited by approximately 42% (Fig. 3B,b). More than 47% of the invading cells were platelet/endothelial cell adhesion molecule-1 immunopositive endothelial cells and/or the progenitor cells (Fig. 3B,a,d). No obvious sign of toxicity was observed in β-HIVS treated mice. These results suggested that β-HIVS suppressed tumor-induced blood vessel formation *in vivo*, at least in part, via a direct action on vascular endothelial and/or progenitor cells. Moreover, spontaneous metastasis of implanted LLC cells to the lung was suppressed to 46% by i.p. administration of β-HIVS (10 mg/kg bodyweight) for 3 weeks (Fig. 4). The bodyweight of the mice did not change significantly and only the weights of original tumor tissues were reduced by 46% (data not shown).

β-HIVS suppressed the phosphorylation and expression of both VEGFR2 and Tie2, and inhibited the growth of both vascular endothelial and progenitor cells. We investigated the molecular mechanism by which β-HIVS inhibited blood vessel formation via a direct effect on the vascular endothelial and/or progenitor cells. Simultaneous inclusion of VEGF and β-HIVS suppressed the proliferation of HUVEC and VPC in a dose-dependent manner, reducing their cell numbers to 20% at 10 μM and 2.5 μM (IC_{50}, 3 and 1 μM), respectively (Fig. 5A). We next examined whether β-HIVS could abrogate the growth stimulating and survival signals by inhibiting the phosphorylation of the angiogenic growth factor receptors in endothelial cells as implicated in the previous report using a reconstituted system in other cell types.[9] As seen in the upper panel of Figure 5(B,a), induction of phosphorylated 230 kDa VEGFR2 due to VEGF treatment was almost completely blocked by pretreatment with 5 μM β-HIVS for 24 h (compare Fig. 5B,a lanes 2 and 3). A similar result was observed with NIH3T3 cells that constitutively overexpressed VEGFR2 (Fig. 5B,b). Surprisingly, levels of VEGFR2 protein expression itself were also significantly reduced following β-HIVS-pretreatment (Fig. 5B,a lane 3 in middle panel). In addition, β-HIVS suppressed the phosphorylation

doi: 10.1111/j.1349-7006.2008.01049.x

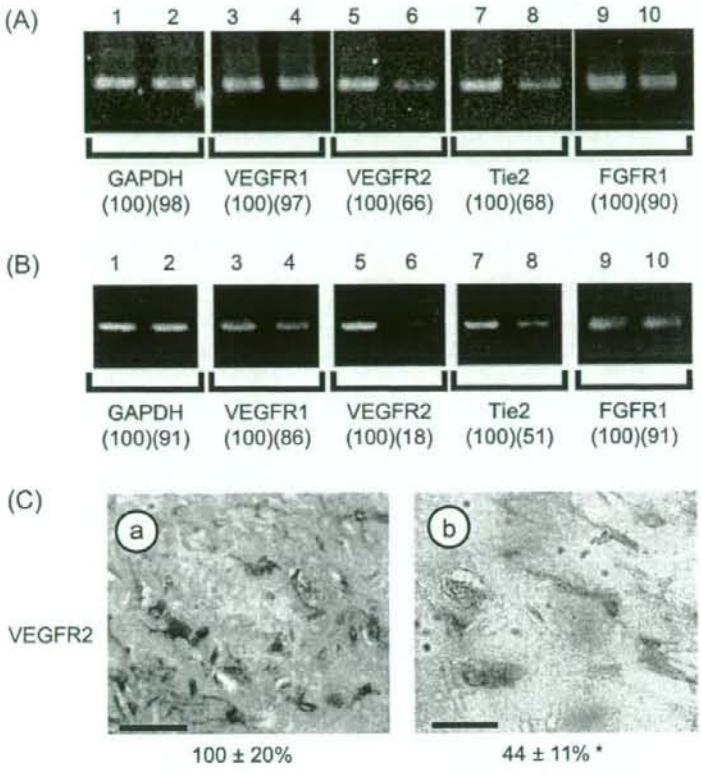

Fig. 7. Suppression of expression of vascular endothelial growth factor receptor (VEGFR) and Tie2 by β-hydroxyisovalerylshikonin (β-HIVS). (A) β-HIVS on mRNA levels of several growth factor receptors. Human umbilical vein endothelial cells (HUVEC) were treated for 24 h with 5 μM β-HIVS. Changes in mRNA levels of the indicated genes were assessed by reverse transcription polymerase chain reaction (RT-PCR). Relative changes in levels were calculated after normalization to levels of *GAPDH* mRNA and are presented as percentages in parentheses under each band. (B) 10 h after HUVEC were treated with 10 nM mithramycin A, changes in mRNA levels were determined by RT-PCR as before. Relative changes in levels were calculated after normalization to levels of *GAPDH* mRNA and are presented as percentages in parentheses under each band. (C) β-HIVS on VEGFR2 expression *in vivo*. Matrigel plugs containing 50 ng/mL vascular endothelial growth factor (VEGF) ± 5 μM β-HIVS were implanted s.c. into mice. A week later, the Matrigel plugs were collected and immunostained with VEGFR2. (a) Minus β-HIVS; (b) plus β-HIVS. Scale lines, 50 μm. The antigen-positive cells in each micrograph were counted and relative changes in numbers are presented as percentages under each photograph. Values represent average ± standard error ($n = 5$). An asterisk indicates a significant difference ($P < 0.05$) from the control. Representative data from a total of nine micrographs (three fields × three mice) are presented. (A–C) Representative results from two or three independent experiments that all gave similar results.

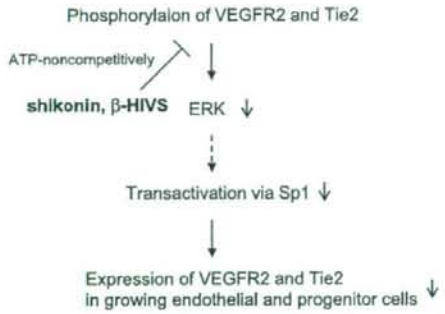

Fig. 8. Hypothetical molecular mechanism. Shikonin and β-hydroxyisovalerylshikonin (β-HIVS) suppress angiogenesis by inhibiting the phosphorylation of vascular endothelial growth factor receptor (VEGFR)2 and Tie2, subsequent inhibition of externally regulated kinases (ERK) and downstream Sp1, culminating in suppression of VEGFR2 and Tie2 expression. ATP, adenosine triphosphate.

and expression of Tie-2 (Fig. 5B,c lane 3 in upper and middle panels, respectively). Under the same condition, levels of GAPDH, an internal control, was unchanged (Fig. 5B, a and c, lane 3 in lower panels).

β-HIVS suppressed MAPK and Sp1-dependent expression of VEGFR2 and Tie2 mRNA. We next investigated the molecular mechanism by which β-HIVS reduced the expression of VEGFR2 and Tie2 in the further detail. β-HIVS abrogated cellular production of phospho-ERK (Fig. 6A lane 3 in upper panel) without changing the levels of total ERK themselves (Fig. 6A lane 3 in lower panel). It has been reported that Sp1 is a downstream transcription factor of ERK and transactivates the promoter of the *VEGFR2* gene.[18] Therefore, we next examined whether β-HIVS might suppress the expression of *VEGFR2* via reduction of Sp1 activity. Treatment of cells with β-HIVS lowered the Sp1 binding and transactivation activities toward the GC box motif within the *VEGFR2* gene promoter (Fig. 6B,C, respectively). β-HIVS also weakly inhibited binding activity of Sp3 transcription factor (Fig. 6B). Comparable reductions were observed in transactivation of the *Tie2* promoter (Fig. 6D) and in the expression of *VEGFR2* and *Tie2* mRNA (Fig. 7A), which were mimicked by mithramycin A, a specific inhibitor of the binding of Sp1/Sp3 to the GC box[19] (Figs 6D and 7B). Both β-HIVS and mithramycin A marginally affected mRNA levels of *VEGFR1* and *FGF receptor 1* (*FGFR1*) (Fig. 7A,B). Inhibition by β-HIVS was partially blocked by Sp1 over-expression in BAEC (Fig. 6E,F). β-HIVS also did not affect the levels of Sp1, VEGF, and Angs-1 and 2. Finally, suppression of the expression of VEGFR2 was also observed during the inhibition of angiogenesis *in vivo*, as assessed by immunostaining of the Matrigel plugs (Fig. 7C). In contrast to the large numbers of VEGFR2-positive cells in control Matrigel plugs (Fig. 7C,a), the number of VEGFR2-positive cells was reduced to 44 ± 11% of the control values (Fig. 7C,b) by inclusion of β-HIVS in the Matrigel plug at 5 μM.

Discussion

In this manuscript, we report the novel molecular mechanism, by which shikonins inhibit tumor angiogenesis. First, we found that β-HIVS exhibits much stronger anti-angiogenic activity than shikonin (Fig. 2A). We anticipate that an isovaleryl group present in the β-HIVS molecule will be found to play an important role in potentiating its anti-angiogenic action compared with that of shikonin. Administration of β-HIVS in mice weakly caused liver damage in the DAS (Supplementary Fig. S1,f), but not in the Matrigel plug assay (data not shown). β-HIVS did not affect epithelial cells constituting chorionic membrane in the CAM assay (Fig. 2B), vasculature in the kidney and tracheal mucosa (Supplementary Fig. S1,b,d), proteinuria (Supplementary Fig. S2A) and pre-existing blood vessels underneath the skin in DAS assay (Fig. 3A). These results suggest that the anti-angiogenic effect of β-HIVS may not be due to cytotoxic effects. Furthermore, neither cellular levels of GAPDH (Figs 5B and 7A) nor ERK (Fig. 6A) was affected by β-HIVS. These results suggest that it affects only proliferating cells that require growth factor stimuli. In Figure 3, because formation of new blood vessels was inhibited the number of platelet/endothelial cell adhesion molecule (PECAM)-negative non-endothelial cells such as macrophages were also thought to be reduced.

β-Hydroxyisovalerylshikonin appears to target the MAPK-Sp1 pathway (Figs 5 and 6) and downstream expression of VEGFR2 and Tie2, thereby inhibiting the growth of vascular endothelial and progenitor cells (Fig. 5A). This is consistent with previous reports that the Ras-MAPK signaling pathway plays an important regulatory role in angiogenesis,[20] and Sp1, a downstream transcription factor of ERK, transactivates the *VEGFR2* promoter.[15,21] On the other hand, the transactivation of *Tie2* promoter by Sp1 is a novel finding. The results in Fig. 6 definitely suggest a role of Sp1 in the expression of both *VEGFR2* and *Tie2*. In Fig. 6(B), lane 3, we could not see an obvious supershift of the Sp1 band, but saw diminishment in the Sp1 band. We think that this is because the anti-Sp1 immunoglobulin G we used for the supershift experiment competitively binds to Sp1's DNA binding domain and therefore that Sp1's bind diminished instead of being uppershifted. The suppressed expression in growth factor receptors is relatively selective for VEGFR2 and Tie2 (Fig. 7A). The effect would be dependent on cell type and experimental conditions. Combination of the current findings and what was reported previously[15,21] suggests that the primary target of β-HIVS is the phosphorylation of several tyrosine kinase receptors in vascular endothelial and/or progenitor cells, and as a secondary effect, the expression of VEGFR2 and Tie2 is suppressed due to reduced MAPK-Sp1 signaling (Fig. 8). It was recently reported that the autocrine VEGF/VEGFR2 signaling pathway is required for homeostasis of blood vessels.[22] Indeed, β-HIVS at higher concentrations (10 μM) induced apoptosis in vascular endothelial cells (Supplementary Fig. S3).

Both VEGF/VEGFR and Ang/Tie2 signaling pathways were important for tumor-associated angiogenesis[5,23] and vasculogenesis.[4] Several compounds have been shown to inhibit either the expression or the phosphorylation of VEGFR2.[24] Most of the clinically-used anti-angiogenic reagents are inhibitors that target VEGFR,[24] whereas a few angiogenesis inhibitors (all-*trans* retinoic acid and 3'-sulfoquinovosyl-1'-monoacylglycerol) have been reported to suppress the expression of Tie2.[12,25] Thus, anti-angiogenic activity targeting Tie2 has been drawing increased attention.[26,27] β-HIVS simultaneously suppressed both the expression and the phosphorylation of VRGFR2 as well as Tie2, suggesting that shikonins would be a novel leading compound to develop an anti-angiogenic reagent with unique bifunctional inhibition of the growth of endothelial cells and vascular remodeling. We are now examining the potential synergistic effect of a combinational use of β-HIVS and other clinically-used VEGFR2 inhibitors in the Matrigel plug assay, based upon our previous finding that the combination of β-HIVS and STI571 suppresses phosphorylation of the BCR/ABL-encoded tyrosine kinase more efficiently than either β-HIVS or STI571 alone in K562 cells.[28]

Acknowledgments

The authors thank Dr K. Umezawa (Keio University, Japan), Dr J. K. Yamashita (Kyoto University, Japan), and Dr R. Nishiwaki (Gifu University, Japan) for providing HUVEC, CCE/nLacZ ES cells and the ERK-specific monoclonal antibody, respectively. This study was supported in part by grants from the Foundation for Promotion of Cancer Research in Japan (to S. K.), and the Chemical Genomics Research Project from RIKEN (to S. K.).

References

1 Carmeliet P. Angiogenesis in life, disease and medicine. *Nature* 2005; **438**: 932–6.
2 Mazitschek R, Giannis A. Inhibitors of angiogenesis and cancer-related receptor tyrosine kinases. *Curr Opin Chem Biol* 2004; **8**: 432–41.
3 Bach F, Uddin FJ, Burke D. Angiopoietin in malignancy. *Eur J Surg Oncol* 2007; **33**: 7–15.
4 Jones N, Iljin K, Dumont DJ, Alitalo K. Tie receptors: new modulators of angiogenic and lymphangiogenic responses. *Nat Rev Mol Cell Biol* 2001; **2**: 257–67.
5 Ferrara N, Kerbel R. Angiogenesis as a therapeutic target. *Nature* 2005; **438**: 967–74.
6 Manley PW, Bold G, Bruggen J *et al*. Advances in the structural biology, design and clinical development of VEGF-R kinase inhibitors for the treatment of angiogenesis. *Biochim Biophys Acta* 2004; **1697**: 17–27.
7 Noble ME, Endicott JA, Johnson LN. Protein kinase inhibitors: insights into drug design from structure. *Science* 2004; **303**: 1800–5.
8 Hashimoto S, Xu M, Masuda Y *et al*. β-Hydroxyisovalerylshikonin inhibits the cell growth of various cancer cell lines and induces apoptosis in leukemia HL-60 cells through a mechanism different from those of Fas and etoposide. *J Biochem* 1999; **125**: 17–23.
9 Hashimoto S, Xu Y, Masuda Y *et al*. β-Hydroxyisovalerylshikonin is a novel and potent inhibitor of protein tyrosine kinases. *Jpn J Cancer Res* 2002; **93**: 944–51.
10 Hisa T, Kimura Y, Takada K, Suzuki F, Takigawa M. Shikonin, an ingredient of *Lithospermun erythrorhizon*, inhibits angiogenesis *in vivo* and *in vitro*. *Anticancer Res* 1998; **18**: 783–90.
11 Botella LM, Sanchez-Elsner T, Sanz-Rodriguez F *et al*. Transcriptional activation of *endoglin* and transforming growth factor-β signaling components by cooperative interaction between Sp1 and KLF6: their potential role in the response to vascular injury. *Blood* 2002; **100**: 4001–410.
12 Suzuki Y, Komi Y, Ashino H *et al*. Retinoic acid controls blood vessel formation by modulating endothelial and mural cell interaction via suppression of Tie2 signaling in vascular progenitor cells. *Blood* 2004; **104**: 166–9.
13 Komi Y, Ohno O, Suzuki Y *et al*. Inhibition of tumor angiogenesis by targeting endothelial surface ATP synthase with sangivamycin. *Jpn J Clin Oncol* 2007; **37**: 867–73.
14 Sawano A, Takahashi T, Yamaguchi S, Aonuma M, Shibuya M. Flt-1 but not KDR/Fll-1 tyrosine kinase is a receptor for placenta growth factor, which is related to vascular endothelial growth factor. *Cell Growth Differ* 1996; **7**: 213–21.
15 Hata Y, Duh E, Zhang K, Robinson GS, Aiello LP. Transcription factors Sp1 and Sp3 alter vascular endothelial growth factor receptor expression through a novel recognition sequence. *J Biol Chem* 1998; **273**: 19294–303.
16 Shimada J, Suzuki Y, Kim SJ, Wang PC, Matsumura M, Kojima S. Transactivation via RAR/RXA–Sp1 interaction: characterization of binding between Sp1 and GC box motif. *Mol Endocrinol* 2001; **15**: 1677–92.
17 Dube A, Akbarali Y, Sato TN, Libermann TA, Oettgen P. Role of the Ets transcription factors in the regulation of the vascular-specific Tie2 gene. *Circ Res* 1999; **84**: 1177–85.
18 Lee JA, Suh DC, Kang JE *et al*. Transcriptional activity of Sp1 is regulated by molecular interactions between the zinc finger DNA binding domain and the inhibitory domain with corepressors, and this interaction is modulated by MEK. *J Biol Chem* 2005; **280**: 28061–71.
19 Suzuki Y, Shimada J, Shudo K, Matsumura M, Crippa MP, Kojima S. Physical interaction between retinoic acid receptor and Sp1: mechanism for induction of urokinase by retinoic acid. *Blood* 1999; **93**: 4264–76.

doi: 10.1111/j.1349-7006.2008.01049.x

20 Wilhelm SM, Carter C, Tang L *et al.* BAY 43–9006 exhibits broad spectrum oral antitumor activity and targets the RAF/MEK/ERK pathway and receptor tyrosine kinases involved in tumor progression and angiogenesis. *Cancer Res* 2004; **64**: 7099–109.
21 Merchant JLM, Todisco A. Sp1 phosphorylation by Erk 2 stimulates DNA binding. *Biochem Biophys Res Commun* 1999; **254**: 454–61.
22 Lee S, Chen TT, Barber CL *et al.* Autocrine VEGF signaling is required for vascular homeostasis. *Cell* 2007; **130**: 691–703.
23 Kobayashi H, Lin PC. Angiopoietin/Tie2 signaling, tumor angiogenesis and inflammatory diseases. *Front Biosci* 2005; **10**: 666–74.
24 Verheul HM, Pinedo HM. Possible molecular mechanisms involved in the toxicity of angiogenesis inhibition. *Nat Rev Cancer* 2007; **7**: 475–85.
25 Mori Y, Sahara H, Matsumoto K *et al.* Downregulation of *Tie2* gene by a novel antitumor sulfolipid, 3'-sulfoquinovosyl-1'-monoacylglycerol, targeting angiogenesis. *Cancer Sci* 2008; **99**: 1063–70.
26 De Palma M, Venneri MA, Galli R *et al.* Tie2 identifies a hematopoietic lineage of proangiogenic monocytes required for tumor vessel formation and a mesenchymal population of pericyte progenitors. *Cancer Cell* 2005; **8**: 211–26.
27 Venneri MA, De Palma M, Ponzoni M *et al.* Identification of proangiogenic TIE2-expressing monocytes (TEMs) in human peripheral blood and cancer. *Blood* 2007; **109**: 5276–85.
28 Masuda Y, Nishida A, Hori K *et al.* β-Hydroxyisovalerylshikonin induces apoptosis in human leukemia cells by inhibiting the activity of a polo-like kinase 1 (PLK1). *Oncogene* 2003; **22**: 1012–23.

Supporting Information

Additional Supporting Information may be found in the online version of this article:

Fig. S1. Morphological changes in the vasculature in the kidney, tracheal mucosa and liver.

Fig. S2. Effect of β-HIVS on proteinuria.

Fig. S3. Induction of apotosis in HUVEC cultures by β-HIVS.

Please note: Wiley-Blackwell are not responsible for the content or functionality of any supporting materials supplied by the authors. Any queries (other than missing material) should be directed to the corresponding author for the article.

nature
cell biology

Differential function of Tie2 at cell–cell contacts and cell–substratum contacts regulated by angiopoietin-1

Shigetomo Fukuhara[1,6], Keisuke Sako[1], Takashi Minami[2], Kazuomi Noda[1], Hak Zoo Kim[3], Tatsuhiko Kodama[2], Masabumi Shibuya[4], Nobuyuki Takakura[5], Gou Young Koh[3] and Naoki Mochizuki[1,6]

Tie2 belongs to the receptor tyrosine kinase family and functions as a receptor for Angiopoietin-1 (Ang1). Gene-targeting analyses of either *Ang1* or *Tie2* in mice reveal a critical role of Ang1–Tie2 signalling in developmental vascular formation. It remains elusive how the Tie2 signalling pathway plays distinct roles in both vascular quiescence and angiogenesis. We demonstrate here that Ang1 bridges Tie2 at cell–cell contacts, resulting in *trans*-association of Tie2 in the presence of cell–cell contacts. In clear contrast, in isolated cells, extracellular matrix-bound Ang1 locates Tie2 at cell–substratum contacts. Furthermore, Tie2 activated at cell–cell or cell–substratum contacts leads to preferential activation of Akt and Erk, respectively. Microarray analyses and real-time PCR validation clearly show the differential gene expression profile in vascular endothelial cells upon Ang1 stimulation in the presence or absence of cell–cell contacts, implying downstream signalling is dependent upon the spatial localization of Tie2.

Vascular development is coordinated by endothelial-specific receptor tyrosine kinases and their ligands: vascular endothelial growth factor (VEGF)–VEGF-receptor (VEGFR), ephrin–Eph receptor, and angiopoietin (Ang)–Tie receptor [1]. The Tie1 and Tie2 receptors constitute the Tie receptor family. Gene-targeting analyses have revealed the essentiality of these vascular endothelial receptor tyrosine kinases for vascular formation [1]. Even after the establishment of vascular network, neovessel formation is observed in ischemic diseases and tumours.

Tie2 maintains the vascular integrity of mature vessels by enhancing endothelial barrier function[2–6] and inhibiting apoptosis of endothelial cells[7–9]. Tie2 functions as a receptor for Ang family proteins (Ang1–4). Mice overexpressing Ang1 develop vessels resistant to inflammatory agent-induced leakage[10,11]. Thus, quiescence of blood vessels is thought to be mediated by Ang1–Tie2 signalling. Tie2 signalling is also suggested to promote cell migration and to be involved in VEGF-induced neovascularization and pathological angiogenesis, as opposed to the maintenance of cell quiescence[12–18]. Consistently, Tie2 is not only tyrosine phosphorylated in the endothelium of normal adult tissues, but is also highly expressed in the endothelium of neovessels of regenerating organs and tumours[19,20].

In the quiescent vessels, the endothelial cells tightly contact each other and do not proliferate[19]. On the other hand, during angiogenesis, the cells that lose cell–cell contacts are allowed to proliferate and migrate, thereby resulting in sprouting and branching from the pre-existing vessels to form neovasculature[19]. At present, it is unknown how Tie2 signalling is involved in both vascular quiescence and angiogenesis. Thus, we investigated Ang1–Tie2 signalling in the presence or absence of vascular endothelial cell–cell contacts.

RESULTS

Ang1 induces the translocation of Tie2 at cell–cell contacts

To first elucidate how Tie2 signalling controls vascular quiescence, we examined the localization of Tie2 in confluent human umbilical vein endothelial cells (HUVECs). Tie2 was broadly expressed on the plasma membrane in unstimulated cells. After stimulation with either cartilage oligomeric matrix protein (COMP)–Ang1, a potent Ang1 variant [14], or native Ang1, Tie2 was accumulated at the cell–cell contacts marked by vascular endothelial cadherin (VE-cadherin) (Fig. 1a and Supplementary Information, Fig. S1a). Similar relocation of Tie2 was observed in human arterial endothelial cells (Supplementary Information, Fig. S1b). The relocation of Tie2 was observed within 5 min after the stimulation, becoming more prominent during 15–45 min (Supplementary Information, Fig. S1c). Tie2 was then gradually endocytosed and disappeared from cell–cell contacts. Re-exposure to COMP–Ang1 6 h after the first stimulation re-induced accumulation of Tie2 at cell–cell contacts (Supplementary Information, Fig. S1d–f). These findings indicate that Ang1 induces relocation of Tie2 to cell–cell contacts, which is also supported by time-lapse imaging of cells expressing Tie2 carboxy-terminally

[1]Department of Structural Analysis, National Cardiovascular Center Research Institute, 5-7-1 Fujishirodai, Suita, Osaka 565-8565, Japan. [2]The Research Center for Advanced Science and Technology, University of Tokyo, Laboratory for System Biology and Medicine, 4-6-1, Komaba, Meguro, Tokyo, 153-8904, Japan. [3]Biomedical Research Center and Department of Biological Sciences, Korea Advanced Institute of Science and Technology, Guseong-dong, Daejeon, 305-701, Korea. [4]Division of Genetics, Institute of Medical Science, University of Tokyo, 4-6-1 Shirokane-dai, Minato-ku, Tokyo 108-8639, Japan. [5]Department of Signal Transduction, Research Institute of Microbial Diseases, Osaka University, 3-1 Yamada-oka, Suita, Osaka, 565-0871, Japan.
[6]Correspondence should be addressed to S.F. or N.M. (e-mails: fuku@ri.ncvc.go.jp; nmochizu@ri.ncvc.go.jp)

Received 3 December 2007; accepted 29 February 2008; published online 20 April 2008; DOI: 10.1038/ncb1714

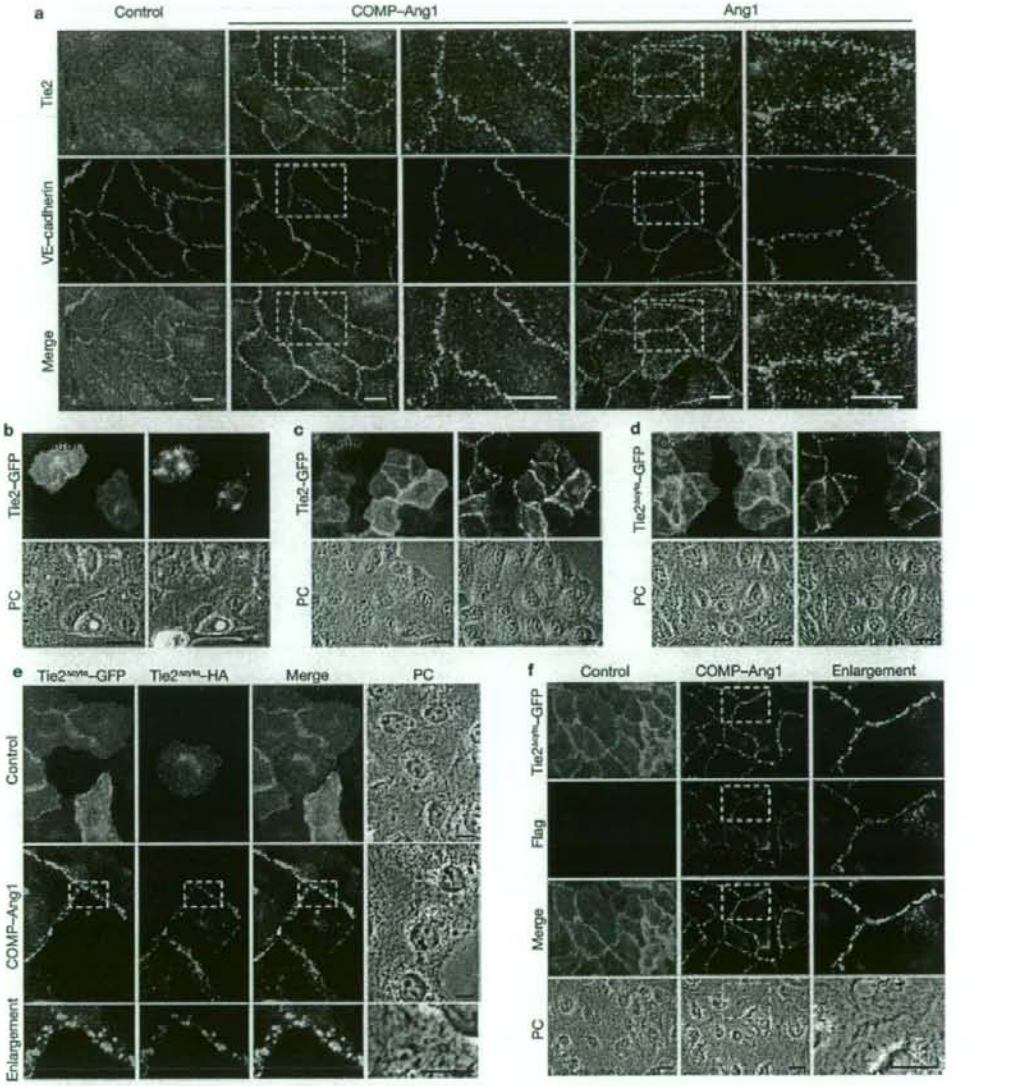

Figure 1 Tie2 is recruited to cell–cell contacts upon Ang1 stimulation in vascular endothelial cells. **(a)** Confluent HUVECs plated on a collagen-coated dish (cells were plated on a collagen-coated dish for the following experiments unless otherwise indicated) were starved in medium 199 containing 0.5% BSA for 3 h and stimulated with vehicle (control), 200 ng ml^{-1} COMP–Ang1, or 600 ng ml^{-1} Ang1 for 20 min (COMP–Ang1 and native Ang1 were used at these concentrations throughout the following experiments unless otherwise indicated). After stimulation, the cells were fixed, immunostained with anti-Tie2 (top) and anti-VE-cadherin (middle) antibodies. Fluorescence images were obtained using an Olympus IX-81 inverted microscope. The boxed areas are enlarged on the right. **(b)** CHO cells transfected with the plasmid expressing Tie2–GFP were starved for 3 h and stimulated with COMP–Ang1. Tie2–GFP (top) and phase-contrast (PC, bottom) images of the Tie2–GFP-expressing cells surrounded by those that do not express Tie2–GFP were time-lapse imaged and analysed by MetaMorph 6.1 software. The images before (left) and 1 h after (right) stimulation are shown. **(c)** Tie2–GFP-expressing cells contacting each other were stimulated with COMP–Ang1 and time-lapse imaged. **(d)** CHO cells transfected with the plasmid expressing Tie2Δcyto–GFP were stimulated with COMP–Ang1 and time-lapse imaged. **(e)** CHO cells were transfected with either the plasmid expressing Tie2Δcyto–GFP or that expressing Tie2Δcyto–HA. The next day, the cells expressing Tie2Δcyto–GFP and those expressing Tie2Δcyto–HA were co-plated and stimulated with either vehicle (control) or COMP–Ang1 for 1 h. After stimulation, the cells were stained with anti-HA antibody. GFP (green), HA (red), the merged images, and the phase-contrast images (PC) are shown. The boxed areas are enlarged at the bottom of each image. **(f)** CHO cells transfected with the vector encoding Tie2Δcyto–GFP were stimulated as described in **e**. To visualize Flag-tagged COMP–Ang1, the stimulated cells were stained with anti-Flag antibody. GFP (green), Flag (red), the merged images (merge), and the phase-contrast images (PC) are shown as labelled on the left. The boxed areas are enlarged in the right panels. The scale bars represent 20 μm (**a**, **b**, **c**, **d**, **f**), and 10 μm (**e**), respectively.

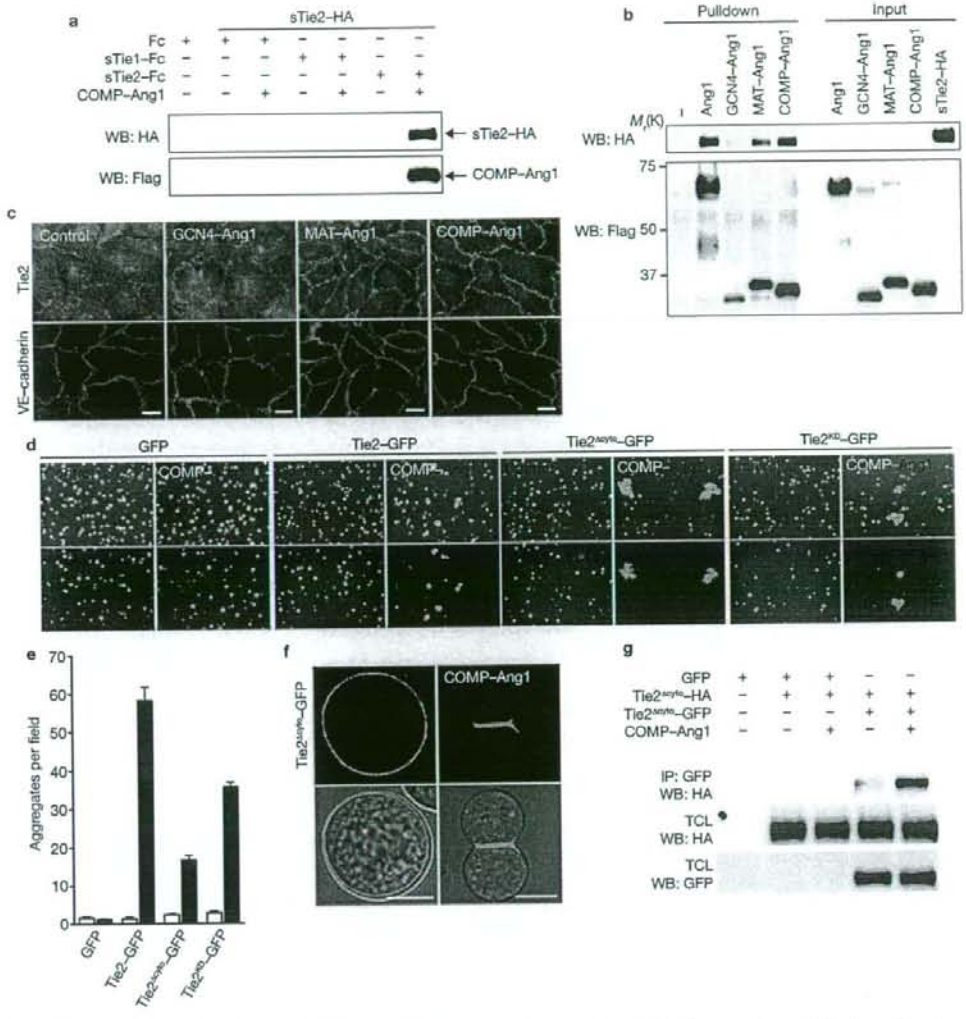

Figure 2 Ang1 induces *trans*-association of Tie2 at cell–cell contacts. (**a**) *In vitro* binding of sTie2–HA to sTie1–Fc or sTie2–Fc. Binding in the presence or absence of COMP–Ang1 was examined as described in Methods. Arrows indicate co-precipitated sTie2–HA and COMP–Ang1 proteins. (**b**) The association of sTie2–HA to sTie2–Fc by Ang1, GCN4–Ang1, MAT–Ang1, or COMP–Ang1 was similarly examined as in **a**. (**c**) Confluent HUVECs were stimulated with vehicle (control), 200 ng ml^{-1} GCN4–Ang1, MAT–Ang1 or COMP–Ang1 for 20 min, and stained with anti-Tie2 (upper panels) and anti-VE-cadherin (lower panels) antibodies. The scale bars represent 20 μm. (**d**) Aggregation of 293F cells in suspension expressing GFP, Tie2–GFP, Tie2Δcyto–GFP and Tie2KD–GFP was induced by vehicle (control; left of each panel) and COMP–Ang1 (right of each panel), as described in Methods. Upper and lower images of each panel show the phase-contrast and GFP images. (**e**) To quantify the cell aggregation observed in **d**, the number of cell aggregates per field of view was counted. An aggregate was defined as cell mass consisting of more than 4 cells. The number of aggregates for cells stimulated with vehicle and COMP–Ang1 is shown as white and black columns, respectively. Data are expressed as mean number ± s.d. of, at least, 10 different fields. (**f**) 293F cells expressing Tie2Δcyto–GFP were incubated with vehicle (control; left column) and COMP–Ang1 (right column). Upper and lower panels show the confocal GFP images merged without or with the DIC images, respectively. The scale bars represent 10 μm. (**g**) 293F cells expressing Tie2Δcyto–HA were suspended with either those expressing Tie2Δcyto–GFP or those expressing GFP, and stimulated with 400 ng ml^{-1} of COMP–Ang1 for 1 h. Cell lysates were immunoprecipitated with anti-GFP antibody. Immunoprecipitates (IP) and aliquots of cell lysate (TCL) were subjected to Western blot analysis (WB) with anti-HA and anti-GFP antibodies. Uncropped images of **a**, **b**, and **g** are shown in Supplementary Information, Fig. S8.

fused with green fluorescent protein (GFP) (Tie2–GFP) (Supplementary Information, Fig. S1g, h and Movie 1).

VEGFR2 is known to associate with VE-cadherin at cell–cell contacts[21,22]. Thus, we assumed that VE-cadherin might be involved in Tie2 relocation to cell–cell contacts. However, Tie2 relocation at cell–cell contacts was still observed in VE-cadherin–depleted HUVECs, while β-catenin disappeared from cell–cell contacts (Supplementary Information, Fig. S2a, c). Tie2 staining at cell–cell contacts was slightly

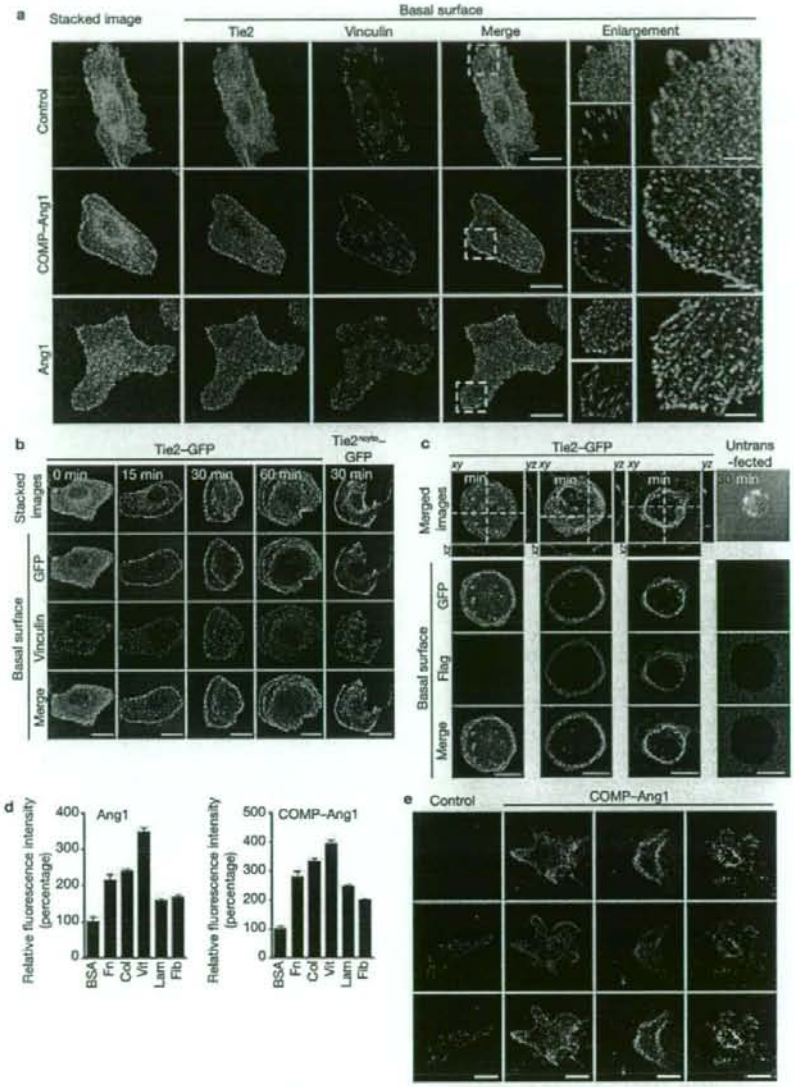

Figure 3 ECM-bound Ang1 anchors Tie2 to cell–substratum contacts in the absence of cell–cell adhesions. (**a**) Sparse HUVECs were stimulated with vehicle (control), COMP–Ang1 or Ang1, and then immunostained with anti-Tie2 and anti-vinculin antibodies. Images were obtained using a confocal microscope. Stacked *xy* images (left), Tie2 (green), vinculin (red) and merged (merge) images of the cell–substratum interface (basal surface) are shown. The boxed areas in the merged images are enlarged (right panels). (**b**) Time course (for the time indicated) of localization of Tie2–GFP and vinculin in CHO cells expressing Tie2–GFP was examined similarly to a. Localization of Tie2Δcyto–GFP after stimulation for 30 min was also examined (left column). (**c**) Localization of COMP–Ang1 (Flag, red) and Tie2–GFP (green) after stimulation with COMP–Ang1 in CHO cells expressing Tie2–GFP was examined similarly to **a**. Untransfected CHO cells were also stimulated with COMP–Ang1, and immunostained with anti-Flag antibody (right column). A DIC image (top) is displayed at the top. (**d**) Binding of Ang1 and COMP–Ang1 to ECM was examined by immunofluorescence analysis as described in Supplementary Methods. Glass-base dishes were coated with BSA (BSA), fibronectin (Fn), collagen (Col), vitronectin (Vit), laminin (Lam), and fibrinogen (Fib), and incubated with Ang1 (left panel) or COMP–Ang1 (right panel). ECM-bound Ang1 and COMP–Ang1 were detected by staining with anti-Flag antibody. Relative immunofluorescence intensity was expressed as a percentage of that detected in a BSA-coated dish. Data are expressed as mean ± s.d. of the fluorescence intensity of 6 different fields. (**e**) Sparse HUVECs expressing both Tie2–GFP and RFP–Crk and those expressing Tie2–GFP were stimulated with COMP–Ang1 or vehicle (control). After stimulation for 20 min, the cells were washed and treated with cytoskeleton stabilizing buffer as described in Methods. The cells expressing Tie2–GFP were immunostained with either anti-vinculin or anti-Flag antibody. GFP (Tie2–GFP), and RFP (RFP–Crk) or Alexa 546 (vinculin or COMP–Ang1) confocal images of the cell–substratum interface, and merged images (bottom) are shown. The scale bars in merged (**a**, **b**, **c**, and **e**) and enlarged images (**a**) represent 20 μm and 5 μm, respectively.

diminished compared to the control cells. Consistently, we found that Tie2 did not co-immunoprecipitate with VE-cadherin in the COMP-Ang1-stimulated HUVECs, although VEGFR2 co-immunoprecipitated with VE-cadherin in those stimulated by VEGF (Supplementary Information, Fig. S2d, e). Furthermore, depletion of platelet and endothelial cell adhesion molecule-1 (PECAM-1) did not affect the relocation of Tie2 to cell–cell contacts (Supplementary Information, Fig. S2b, c). These results indicate that VE-cadherin and PECAM-1 are not essential for Tie2 localization at cell–cell contacts, although cell adhesions by these molecules may affect the localization of Tie2 by stabilizing cell–cell contacts.

We hypothesized that the interaction of Tie2 expressed in adjoining cells might be required for the accumulation of Tie2 at cell–cell contacts. We employed Chinese hamster ovary (CHO) cells that do not express endogenous Tie2 and CHO cells expressing Tie2–GFP. By monitoring Tie2–GFP upon COMP-Ang1 stimulation, we could distinguish the dynamics of Tie2–GFP in the presence or absence of Tie2 expression between adjoining CHO cells. Tie2–GFP was internalized upon stimulation with COMP-Ang1 when a Tie2–GFP-expressing cell was surrounded by wild-type CHO cells (Fig. 1b and Supplementary Information, Movie2). In contrast, COMP-Ang1 stimulation induced Tie2–GFP translocation to the cell–cell borders between adjacent cells expressing Tie2–GFP, although Tie2–GFP was homogeneously expressed on the plasma membrane before the stimulation (Fig. 1c and Supplementary Information, Fig. S2f and Movie3). Notably, Tie2–GFP lacking the cytoplasmic domain of Tie2 (Tie2Δcyto–GFP) relocated to the borders between adjacent cells expressing Tie2Δcyto–GFP (Fig. 1d and Supplementary Information, Movie 4). To further test the effect of the extracellular domain of Tie2 between adjoining cells on the accumulation of Tie2 at cell–cell contacts, CHO cells expressing Tie2Δcyto–GFP and those expressing Tie2Δcyto–HA (a mutant Tie2 lacking the cytoplasmic domain tagged with HA) were co-plated and stimulated with COMP-Ang1. In the unstimulated cells, both Tie2Δcyto–GFP and Tie2Δcyto–HA were broadly expressed on the plasma membrane without any colocalization. Once stimulated with COMP-Ang1, Tie2Δcyto–GFP and Tie2Δcyto–HA colocalized at the cell–cell borders between cells expressing Tie2Δcyto–GFP and cells expressing Tie2Δcyto–HA (Fig. 1e). Interestingly, COMP-Ang1 was also detected at the cell–cell borders where Tie2Δcyto–GFP localized (Fig. 1f). Collectively, these findings suggest that Ang1 induces *trans*-association of Tie2 at cell–cell contacts independently of its intracellular signalling.

Internalization was further analysed by a confocal microscope. In Tie2–GFP-expressing CHO cells surrounded by wild-type CHO cells, Tie2–GFP was clearly internalized upon COMP-Ang1 stimulation, while in either Tie2Δcyto–GFP-expressing CHO cells or kinase-negative Tie2–GFP (Tie2KD–GFP)-expressing CHO cells, Tie2 was not internalized (Supplementary Information, Fig. S2g). These data indicate that endocytosis of Tie2 is triggered by its intracellular signalling, and suggest that Ang1-induced localization of Tie2 at cell–cell contacts depends upon the balance between *trans*-association of activated Tie2 and the internalization of Tie2.

Trans-association of Tie2 induced by oligomerized Ang1

To explore whether the *trans*-association of Tie2 is provoked by oligomerized Ang1, we first biochemically analysed the association of Tie2 using recombinant Tie proteins. We tested the association of immunoglobulin Fc-domain tagged extracellular domain of either Tie1 or Tie2 with the HA-tagged extracellular domain of Tie2, as explained in Supplementary Fig. 3a and 3b. HA-tagged Tie2 bound to sTie2–Fc but not sTie1–Fc in the presence of COMP-Ang1 (Fig. 2a). We then tested the association of sTie2–HA with sTie2–Fc in the presence of various forms of Ang1 (GCN4–Ang1, dimer; native Ang1 and MAT–Ang1, tetramer; COMP–Ang1, pentamer)[14]. The association of sTie2–HA with sTie2–Fc was induced by native Ang1, MAT–Ang1, and COMP–Ang1, which can form multimers of Ang1, but not by GCN4–Ang1 (Fig. 2b). Consistently, multimerized Ang1 induced the relocation of Tie2 at cell–cell contacts (Fig. 2c).

We further tested the possibility of Ang1-mediated bridging of Tie2 by using 293 cells in suspension (293F). Tie2–GFP-expressing 293F cells but not GFP-expressing 293F cells aggregated upon COMP–Ang1 and native Ang1 stimulation (Fig. 2d, e and Supplementary Information, Fig. S3c, d). The number of aggregates in Tie2–GFP-expressing cells increased more than in Tie2Δcyto–GFP-expressing cells and Tie2KD–GFP-expressing cells that were resistant to internalization of Tie2 (Fig. 2e and Supplementary Information, Fig. S2g). In contrast, the size of the aggregates was increased in Tie2Δcyto–GFP-expressing cells and Tie2KD–GFP-expressing cells compared to Tie2–GFP-expressing cells (Supplementary Information, Fig. S3e), suggesting that intracellular signalling may affect Ang1-mediated Tie2 *trans*-association probably through Tie2 internalization.

In the aggregated cells, Tie2Δcyto–GFP clearly localized at the sites of cell–cell contacts (Fig. 2f). Similar localization of Tie2Δcyto–GFP at cell–cell contacts was observed in a murine pro-B cell line, BaF3 cells, stably expressing Tie2Δcyto–GFP (BaF–Tie2ΔcytoGFP) upon COMP–Ang1 stimulation (Supplementary Information, Fig. S3h). VEGF did not induce aggregation of 293F cells expressing VEGFR2, although VEGFR2 is reported to localize to cell–cell contacts [21,23](Supplementary Information, Fig. S3f, g). When 293F cells expressing Tie2Δcyto–GFP and those expressing Tie2Δcyto–HA were co-cultured in suspension and stimulated with COMP–Ang1, both Tie2 were co-immunoprecipitated (Fig. 2g). Furthermore, when BaF–Tie2ΔcytoGFP cells and BaF3 cells stably expressing Tie2Δcyto–HA (BaF–Tie2ΔcytoHA) were mixed and stimulated with COMP–Ang1 in suspension, both truncated forms of Tie2 were also co-immunoprecipitated (Supplementary Information, Fig. S3i). These results together with biochemical data and the co-localization of Tie2 lacking its cytoplasmic domain (Fig. 1e) indicate the *trans*-association of Tie2 occurs at cell–cell contacts upon oligomerized Ang1 stimulation.

Tie2 localizes to cell–substratum contacts in the absence of cell–cell contacts

We next examined Ang1-induced localization of Tie2 in sparse HUVECs. In subconfluent HUVECs, Tie2 was preferentially recruited to cell–cell contacts upon COMP–Ang1 stimulation (Supplementary Information, Fig. S4a). However, when stimulated in the absence of cell–cell contacts, Tie2 localized to the periphery of the extended membrane that was close to but different from vinculin- and paxillin-positive focal complexes (FCs) (Fig. 3a and Supplementary Information, Fig. S4b). We further investigated COMP–Ang1-induced localization of Tie2–GFP in CHO cells. Tie2–GFP was localized to the periphery at 15, 30 and 60 min after stimulation. We noticed additional GFP-positive lines at cell–substratum contacts in the cells stimulated for 30 min and 60 min, reflecting the footprints of membrane extension during cell movement (Fig. 3b).

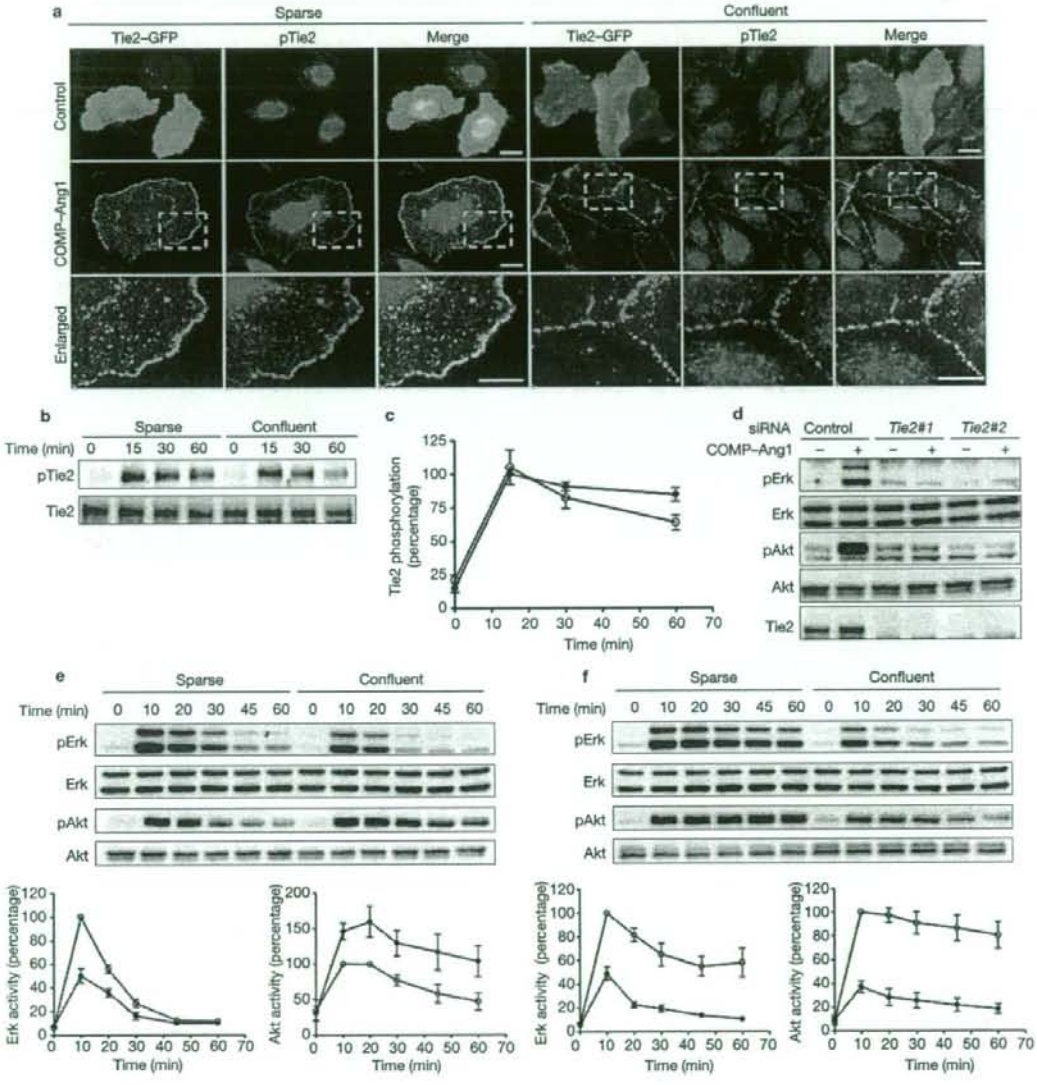

Figure 4 *Trans*-association of Tie2 leads to the preferential activation of Akt. (**a**) Sparse and confluent HUVECs were transfected with the plasmid encoding Tie2–GFP, stimulated with either vehicle (control) or COMP–Ang1, and immunostained with an anti-phospho Tie2 (pTie2) antibody. Images of Tie2–GFP (green), pTie2 (red), and the merged images (merge) are shown. The boxed areas in the panels are enlarged at the bottom of each image. The scale bars in the merged and the enlarged images represent 20 and 5 μm, respectively. (**b**) Sparse and confluent HUVECs were starved and stimulated with COMP–Ang1 for the time (min) indicated at the top. Cell lysates were immunoprecipitated with anti-Tie2 antibody. Immunoprecipitates and aliquots of cell lysate were subjected to western blot analysis with anti-phosphotyrosine (pTie2) and anti-Tie2 (Tie2) antibodies. (**c**) Phosphorylated Tie2 observed in **b** was quantified. Tie2 phosphorylation represents the ratio of phosphorylated Tie2 to total Tie2 as a percentage of the ratio in the sparse cells stimulated for 15 min. Values are expressed as means ± s.d. from five independent experiments. (**d**) HUVECs transfected with control siRNA (control) or with two independent siRNAs targeting different sequences of *Tie2* (Tie2 No.1 and Tie2 No.2) were starved and stimulated with vehicle (–) and COMP–Ang1 (+) for 15 min. Cell lysates were subjected to immunoblot analysis for analysing Erk and Akt phosphorylation. (**e**) Sparse and confluent HUVECs were stimulated with COMP–Ang1 for the time (min) indicated at the top. Activation of Erk and Akt was analysed. Graphs at the bottom left and right panels show time course of Erk and Akt activation of the sparse cells (open circle) and the confluent cells (filled circle) in response to COMP–Ang1. Erk or Akt activity represents the ratio of phospho-Erk or phospho-Akt to total Erk or total Akt as a percentage of the ratio observed in sparse cells stimulated for 10 min, respectively. Values are expressed as means ± s.d. from five independent experiments. (**f**) Sparse (open circle) and confluent (filled circle) HUVECs were stimulated with growth media and analysed. Uncropped images of **b**, **d**, **e**, **f** are shown in Supplementary Information, Fig. S8.

Likewise, in Tie2Δcyto–GFP-expressing CHO cells, Tie2Δcyto–GFP was found at cell–substratum contacts, indicating the requirement of the extracellular domain of Tie2 for this localization. These Tie2–GFP positive structures at cell–substratum contacts were located close to, but apparently different from, vinculin-marked FCs or focal adhesions (FAs) (Supplementary Information, Fig. S4c). To identify the cell matrix junctions where Tie2 localizes, we carefully compared Tie2–GFP with those of various markers for FCs and FAs in HUVECs plated on fibronectin- and collagen-coated dishes after COMP–Ang1 stimulation. Tie2–GFP at cell–substratum contacts colocalized with none of these markers including vinculin, paxillin, VASP, and talin (Supplementary Information, Fig. S5a–g). Collectively, these results indicate that upon stimulation with Ang1, Tie2 is recruited to the cell periphery and anchored to substratum contacts that are different from FCs and FAs. This is further supported by time-lapse imaging using HUVECs expressing Tie2–GFP and CHO cells expressing either Tie2–GFP or Tie2Δcyto–GFP upon COMP–Ang1 stimulation (Supplementary Information, Movie 6 and 7).

$\alpha_5\beta_1$ integrin associates with fibronectin fibrils to form distinct adhesive structures from FCs and FAs, namely fibrillar adhesions (FBs) where fibrinogenesis occurs[24,25]. Since Cascone *et al.* has reported that Tie2 constitutively associates with $\alpha_5\beta_1$ integrin that binds to fibronectin[26], we examined whether Tie2 localizes at FBs. When Tie2–GFP– or HA-tagged Tie2 (Tie2–HA)–expressing HUVECs plated on a fibronectin-coated dish were stimulated with COMP–Ang1, Tie2 did not colocalize with FB markers (α_5 integrin, assembled fibronectin fibrils and exogenously expressed GFP–tensin) (Supplementary Information, Fig. S5h–j). In addition, depletion of α_5 integrin by siRNA did not affect COMP–Ang1-induced Tie2 localization at cell–substratum contacts (Supplementary Information, Fig. S6a–d). Depletion of another integrin, $\alpha_v\beta_3$, did not alter COMP–Ang1-induced relocation of Tie2 to peripheral cell–substratum contacts (Supplementary Information, Fig. S6 a–c).

We assumed that Ang1 might anchor Tie2 to extracellular matrix (ECM). When Tie2–GFP-expressing CHO cells were sparsely cultured on collagen-coated dishes and stimulated with COMP–Ang1, Tie2–GFP and FLAG-tagged COMP–Ang1 were clearly colocalized at the periphery and bottom of the cells at 5 min after stimulation, with the appearace of a ring (Fig. 3c). After 30 min, we noticed that Ang1 was detected not only with Tie2–GFP but also on the dish surface where the cell was not present (Fig. 3c and Supplementary Information, Fig. S6e), suggesting that Ang1 can bind to ECM. Indeed, Ang1 and COMP–Ang1, but not control protein, could bind to fibronectin, collagen, and vitronectin with high affinity, and bind weakly to laminin and fibrinogen as demonstrated by an ECM–Ang1 binding assay (Fig. 3d and Supplementary Information, Fig. S6f). Adhesive structures formed at cell–substratum contacts such as FCs and FAs are resistant to detergent (0.5% Triton-X100)[27,28]. Whereas Tie2–GFP but not RFP–Crk disappeared upon detergent addition without pretreatment of COMP–Ang1, pretreatment of COMP–Ang1 preserved Tie2–GFP at the bottom of cells as well as RFP–Crk and vinculin (Fig. 3e). These results suggest that Tie2 is anchored by ECM-bound Ang1 to cell–substratum contacts to form novel detergent-resistant adhesive structures, which are different from FCs, FAs and FBs.

Preferential activation of Erk and Akt in the absence and presence of cell–cell contacts upon Ang1 stimulation

We investigated the biological significance of *trans*-associated Tie2 at cell–cell contacts and cell–substratum contact-anchored Tie2 upon Ang1 stimulation. Tie2 under both conditions was phosphorylated at either cell–cell contacts or cell–substratum contacts (Fig. 4a). The extent of Tie2 phosphorylation in HUVECs by COMP–Ang1 did not depend upon the presence of cell–cell contacts (Fig. 4b, c).

Among Tie2-mediated signalling factors[4,19], Akt and Erk are suggested to be important for cell survival, and cell migration and proliferation, respectively[8,29,16,30,31]. We therefore checked the requirement of Tie2 in Ang1-induced Erk and Akt activation in HUVECs, because Ang1 is known to mediate some biological functions through integrins [32,33]. Ang1-dependent phosphorylation of both Erk and Akt in confluent and sparse HUVECs was abolished by depletion of Tie2 (Fig. 4d and data not shown). Under either sparse or confluent culture conditions, COMP–Ang1 induced Erk phosphorylation, which peaked at 10 min after stimulation and declined to the basal level by 45 min (Fig. 4e). However, the maximum level of Erk phosphorylation in the confluent cells was reduced to approximately 50% of that in the sparse cells (Fig. 4e). In clear contrast, the maximum increase in Akt phosphorylation was significantly higher in the confluent cells than in the sparse cells (Fig. 4e), indicating that endothelial cell–cell adhesions positively regulate the Tie2-mediated Akt pathway. We noticed that this preferential activation of Akt was a Tie2-specific signal in the confluent cell culture, because both Erk and Akt activation was suppressed when the endothelial cells were stimulated with growth media in the presence of cell–cell contacts (Fig. 4f).

Activation of Erk by Tie2 at cell–substratum contacts is partly dependent upon focal adhesion kinase and involved in endothelial cell migration

To further explore how Tie2-mediated signalling in isolated cells is influenced by its targeting to cell–substratum contacts, HUVECs were stimulated with COMP–Ang1 under either suspended or substratum-attached conditions. While Tie2 phosphorylation and subsequent Akt activation were comparable between these conditions, Erk activation was higher in substratum-attached cells (Fig. 5a). Similar results were obtained using BaF3 cells stably expressing Tie2 (BaF–Tie2) (Supplementary Information, Fig. S7a–c). These findings suggest that Erk activation by Ang1–Tie2 requires the contacts between cells and substratum, as previously reported for other receptor tyrosine kinases[34,35].

We hypothesized that Ang1–Tie2 at cell–substratum contacts cooperatively function with integrin signalling complexes to induce Erk activation, although Tie2 localized to cell–substratum contacts besides FCs, FAs and FBs. To test this possibility, we examined whether ECM-anchored Ang1 induces Tie2 signalling and modulates integrin adhesions. In HUVECs adhering to a collagen-coated dish, Tie2 diffusely localized at bottom surface of the cells. In clear contrast, Tie2 was found to be punctate and phosphorylated at cell–substratum contacts when the cells were attached to a collagen- and COMP–Ang1-coated dish (Supplementary Information, Fig. S7d, e), indicating the capability of ECM-anchored Ang1 to stimulate Tie2. HUVECs adhering to collagen- and COMP–Ang1-coated substratum exhibited enhanced vinculin accumulation at the most peripheral region of the cells, compared with the cells attached to collagen, as analysed by line-scanning of immunofluorescence intensity (Fig. 5b, c). Consistently, fewer stress fibres and more lamellipodia were observed in the presence of COMP–Ang1 (Supplementary Information, Fig. S7f). These data reveal that Ang1–Tie2 signalling at cell–substratum contacts induces FC formation.

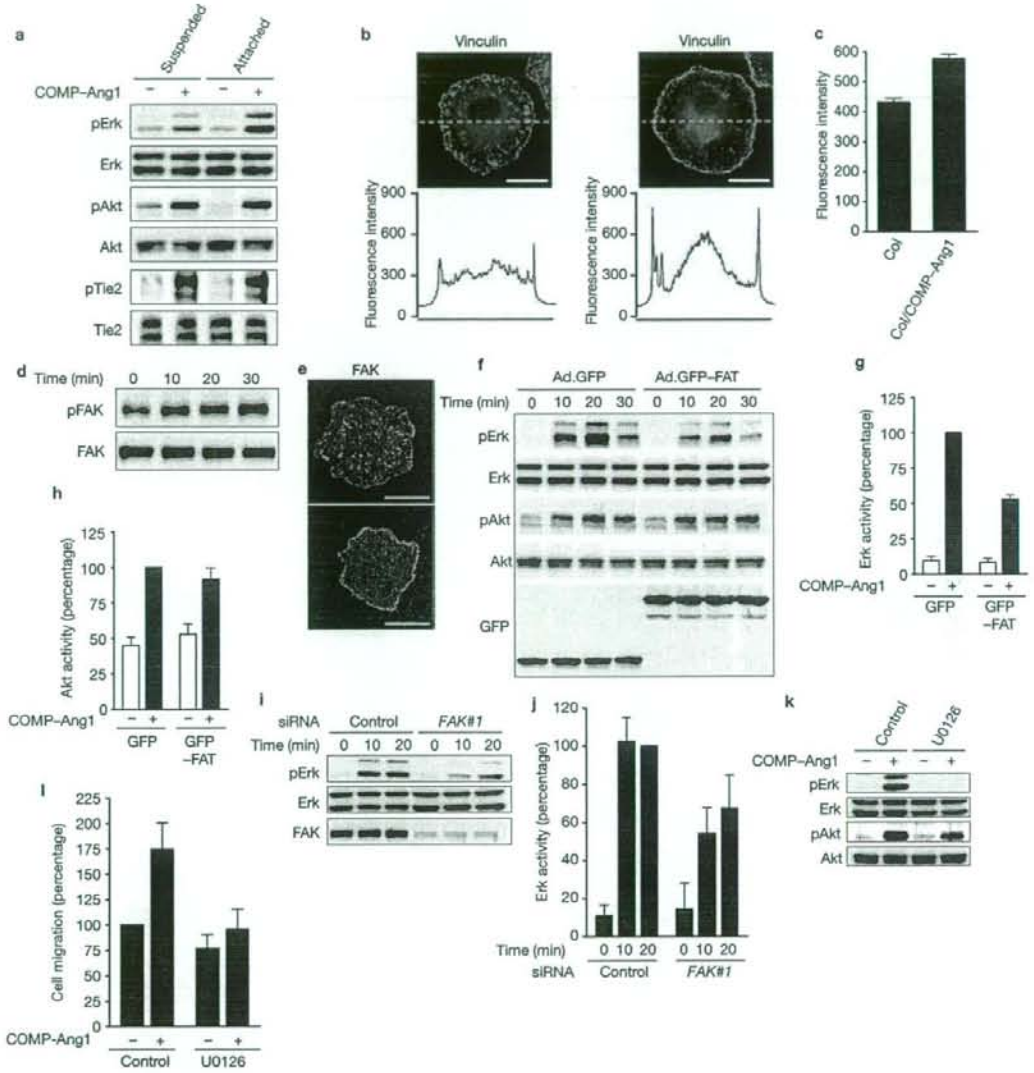

Figure 5 Activation of Erk by Tie2 at cell–substratum contacts partly depends upon FAK and is involved in endothelial cell migration. (**a**) Suspended HUVECs and cells adhered on a as described in Supplementary Methods. (**b**) HUVECs were placed on the COMP-Ang1–unbound collagen-coated dish (Col) or COMP-Ang1–bound collagen-coated dish (Col and COMP-Ang1) for 30 min, and immunostained with anti-vinculin antibody. Focal complexes were analysed by line intensity scan using MetaMorph 6.1 software (fluorescence intensity along the dotted line indicated, bottom panels). (**c**) Quantification of the Results of **b**. Values are expressed as means ± s.d. of fluorescence intensity relative to vinculin at the cell periphery (Col, $n = 60$; Col & COMP-Ang1, $n = 66$). (**d**) Sparse HUVECs starved for 6 h were stimulated with COMP-Ang1 for different times (min). Immunoprecipitates and cell lysate were subjected to western blot analysis with anti-phosphotyrosine (pFAK) and anti-FAK (FAK) antibodies, respectively. (**e**) Localization of FAK was examined similarly to **b**. (**f**) Sparse HUVECs plated on a collagen-coated dish were infected with adenovirus vector encoding either GFP or GFP-FAT as described in Supplementary Information, Methods. Cells stimulated with COMP-Ang1 for 20 min were analysed for Erk and Akt activation. (**g**, **h**) Phosphorylation of Erk (**g**) and Akt (**h**) in **f** was quantified. Values are expressed as means ± s.d. from five independent experiments. (**i**) Effect of knockdown of FAK on Erk activation was examined in control siRNA (control) or *FAK* siRNA-treated HUVECs (FAK No.1). (**j**) Quantification of the results of **i**. Values are expressed as means ± s.d. from 6 independent experiments. (**k**, **l**) MEK–Erk inhibition results in decreased migration of sparse HUVECs stimulated with COMP-Ang1. 20 μM U0126 (a MEK inhibitor) inhibits COMP-Ang1-induced Erk, but not Akt activation (**k**). Migration of HUVECs was analysed as described in Supplementary Methods (**l**). Values are expressed as the mean ± s.d. from 5 independent experiments. The scale bars represent 20 μm (**b**, **e**). Uncropped images of **a**, **d**, **f**, **i**, **k** are shown in Supplementary Information, Fig. S8.

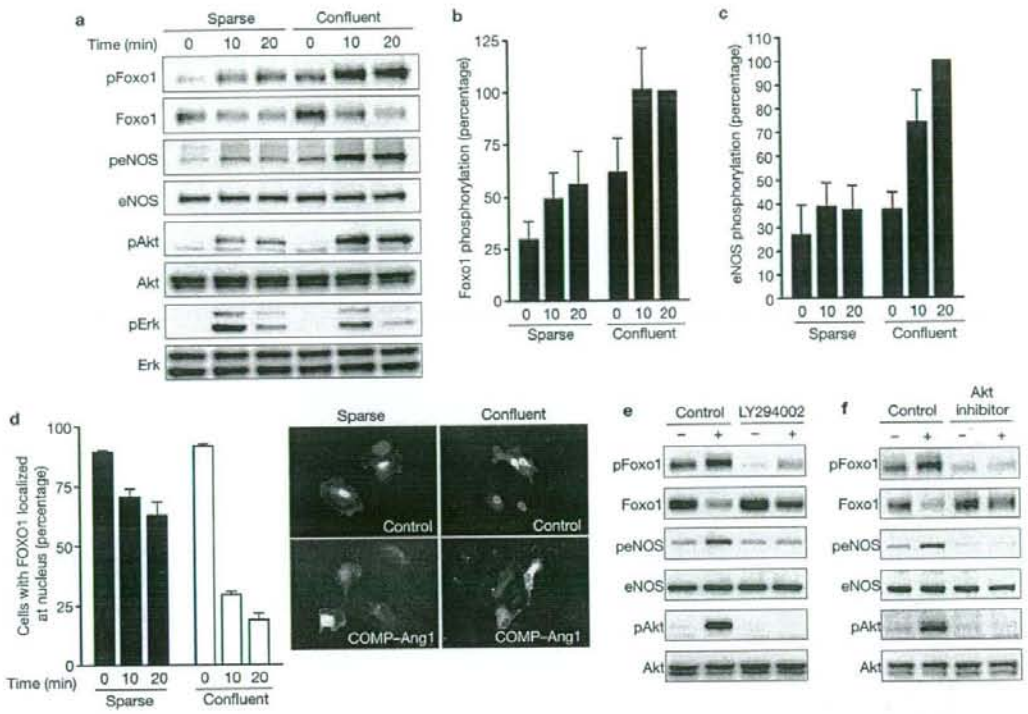

Figure 6 The presence of cell–cell contacts determines the preferential activation of Akt and subsequent phosphorylation of Foxo1 and eNOS. (**a**) Sparse and confluent HUVECs were starved and stimulated with COMP-Ang1. Cell lysates were analysed for phosphorylation of Foxo1, eNOS, Akt, and Erk. Note that Foxo1 and eNOS are more phosphorylated in the confluent cells than in the sparse cells. (**b**) COMP-Ang1-induced phosphorylation of Foxo1 observed in **a** was quantified. Foxo1 phosphorylation represents the ratio of phosphorylated Foxo1 to total Erk protein as a percentage of the ratio in the confluent cells stimulated for 20 min. Erk protein but not Foxo1 was used as normalization for protein loading, because anti-Foxo1 antibody does not recognize phosphorylated Foxo1. Values are expressed as means ± s.d. from seven independent experiments. (**c**) COMP-Ang1-induced phosphorylation of eNOS observed in **a** was quantified. eNOS phosphorylation represents the ratio of phosphorylated eNOS to total eNOS as a percentage of the ratio in the confluent cells stimulated for 20 min. Values are expressed as means ± s.d. from seven independent experiments. (**d**) Sparse and confluent HUVECs transfected with a plasmid encoding GFP–Foxo1 were starved for 6 h and stimulated with COMP-Ang1 for the time (min) as indicated. After fixation in methanol, the number of cells with GFP–Foxo1 localized at nucleus was counted and expressed as a percentage relative to total number of cells. At least 100 GFP-positive cells were scored for each treatment. Values are expressed as means ± s.d. from three independent experiments. Representative images of subcellular localization of GFP–Foxo1 in sparse (left) and confluent (right) cells are shown on the bottom. Upper and lower panels show the images in cells stimulated with vehicle or COMP-Ang1 for 20 min. (**e**, **f**) Confluent HUVECs were pre-treated with 20 μM LY294002 for 30 min (**e**) or 8 μM Akt inhibitor for 5 min (**f**) and subsequently stimulated with vehicle (–) or COMP-Ang1 (+) for 20 min. The effect of both inhibitors on COMP-Ang1-induced phosphorylation of Foxo1, eNOS, and Akt was examined. Uncropped images of **a**, **e**, and **f** are shown in Supplementary Information, Fig. S8.

Focal adhesion kinase (FAK) localizing at FCs and FAs mediates signalling by integrins and growth factor receptors to activate Erk[36,37]. Previously, it has been reported that Ang1 activates FAK to induce endothelial cell sprouting[13]. Thus, we tested the involvement of FAK in Erk activation downstream of cell–substratum contact-anchored Tie2 upon Ang1 stimulation. COMP-Ang1 induced tyrosine phosphorylation and accumulation of FAK to FCs in HUVECs (Fig. 5d and Supplementary Information, Fig. S7g) and increased the FAK-positive FC assembly as well as vinculin (Fig 5b, e). Consistent with the idea that the focal-adhesion-targeting domain of FAK (FAT) displaces FAK from FCs and FAs[36], overexpression of RFP-tagged FAT (RFP–FAT) perturbed the localization of FAK to FCs and FAs in HUVECs (Supplementary Information, Fig. S7h). Tie2 localization at peripheral cell–substratum contacts upon COMP-Ang1 stimulation was not influenced by overexpression of FAT (Supplementary Information, Fig. S7i). We next investigated the effect of FAT on Tie2-mediated intracellular signalling. Overexpression of GFP-tagged FAT (GFP–FAT) significantly but not completely inhibited COMP-Ang1-induced Erk activation (Fig. 5f, g). In clear contrast, overexpression of FAT did not alter COMP-Ang1-induced Akt activation (Fig. 5f, h). Furthermore, depletion of FAK by siRNAs partly inhibited COMP-Ang1-induced Erk activation (Fig. 5i, j and Supplementary Information, Fig. S7j, k). Collectively, these results indicate that Erk activation by Tie2 anchored to cell–substratum contacts is ascribed partly to FAK.

Erk signalling is known to be involved in endothelial cell migration[38]. Thus, we examined the role of Erk in cell migration by Ang1–Tie2 at cell–substratum contacts. Cell motility was enhanced when HUVECs

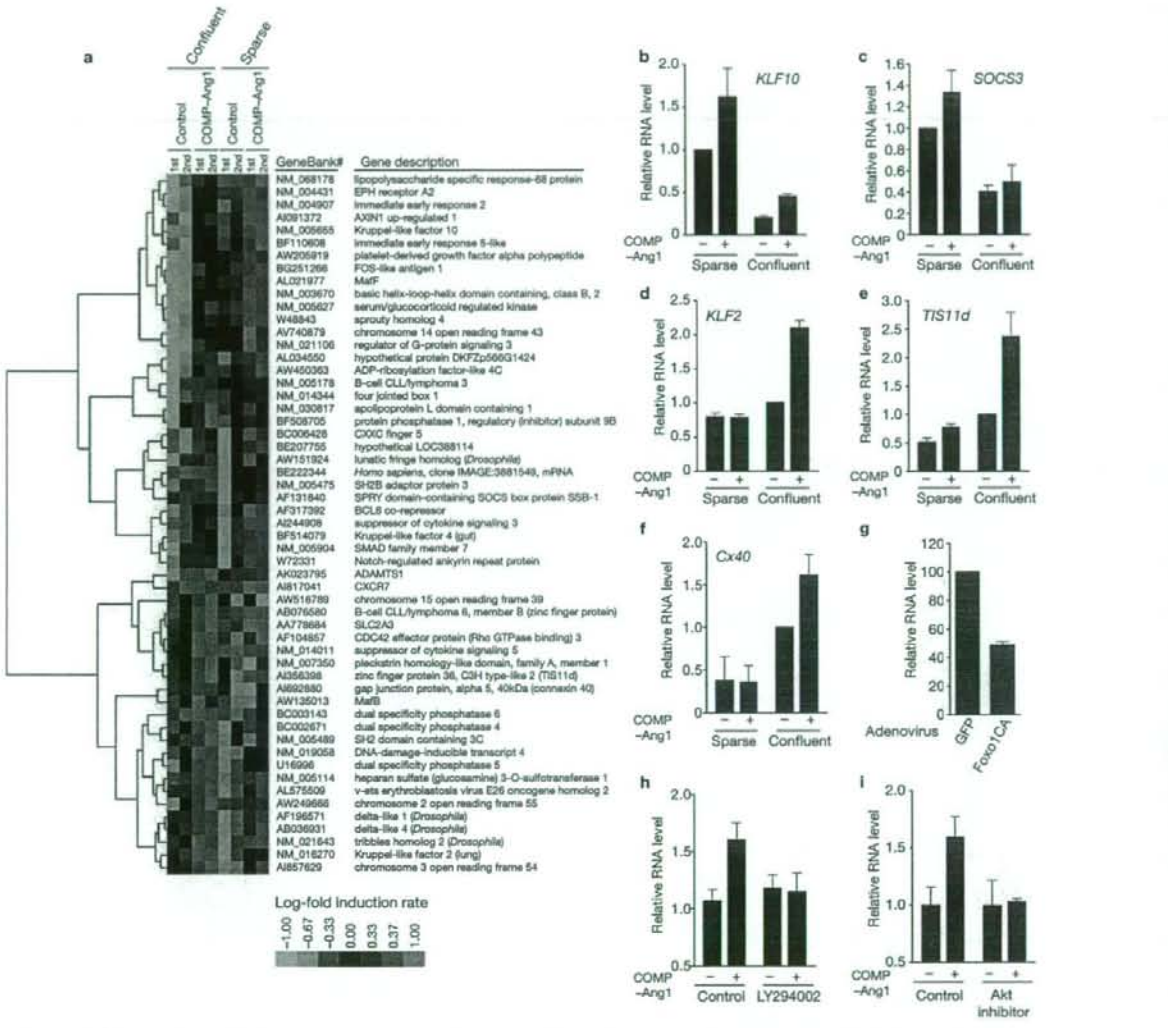

Figure 7 Ang1 stimulation leads to a distinct pattern of gene expression in HUVECs in the presence or absence of cell–cell contacts. (**a**) Total RNA was purified from confluent and sparse HUVECs stimulated with vehicle (control) or COMP–Ang1 for 1 h, and subjected to Affymetrix microarray analysis, as described in Methods. Genes corresponding to the criteria described in Methods were subjected to the cluster analysis. The results from two independent microarray analyses are displayed. Red and green represent higher and lower expression than the median for that particular gene, respectively. Color intensity is related to the difference with the median (black). (**b–f**) Total RNA was purified from confluent and sparse HUVECs stimulated with vehicle (–) or COMP–Ang1 (+) for 1 h, and expression levels of *KLF10* (**b**), *SOCS3* (**c**), *KLF2* (**d**), *TIS11d* (**e**) and *Cx40* (**f**) were analysed by real-time RT–PCR analysis as described in Supplementary Information, Methods. Bar graphs show relative RNA levels of each gene normalized to GAPDH levels. RNA levels are expressed relative to that in sparse (**b**, **c**) or confluent (**d–f**) cells stimulated with vehicle. Values are expressed as means ± s.d. from more than three independent experiments. (**g**) Total RNA was isolated from confluent HUVECs infected with adenovirus vectors encoding either GFP (GFP) or a constitutively active mutant of Foxo1 (Foxo1CA). Expression levels of *Cx40* were analysed as described for **f**, and expressed as a percentage relative to that in cells infected with GFP-encoding adenovirus vector. (**h**) Confluent HUVECs were stimulated with COMP–Ang1 in the presence (LY294002) or absence (control) of LY294002 as described in the legend of Fig. 6e. Expression levels of *Cx40* were analysed as described for **f**. Data are means ± s.d. of triplicate samples, and similar results were obtained in three independent experiments. (**i**) Confluent HUVECs were stimulated with COMP–Ang1 in the presence (Akt inhibitor) or absence (control) of Akt inhibitor as described in the legend of Fig. 6f. Expression levels of *Cx40* were analysed and expressed as described for **h**.

were placed on collagen- and COMP–Ang1-coated transwell filters, compared with cells adhering to collagen-coated filters. This enhanced cell motility was cancelled by inhibiting Erk using U0126, a MEK inhibitor (Fig. 5k, l). These findings suggest that Ang1–Tie2 at cell–substratum contacts regulates endothelial cell migration through the Erk signalling pathway.

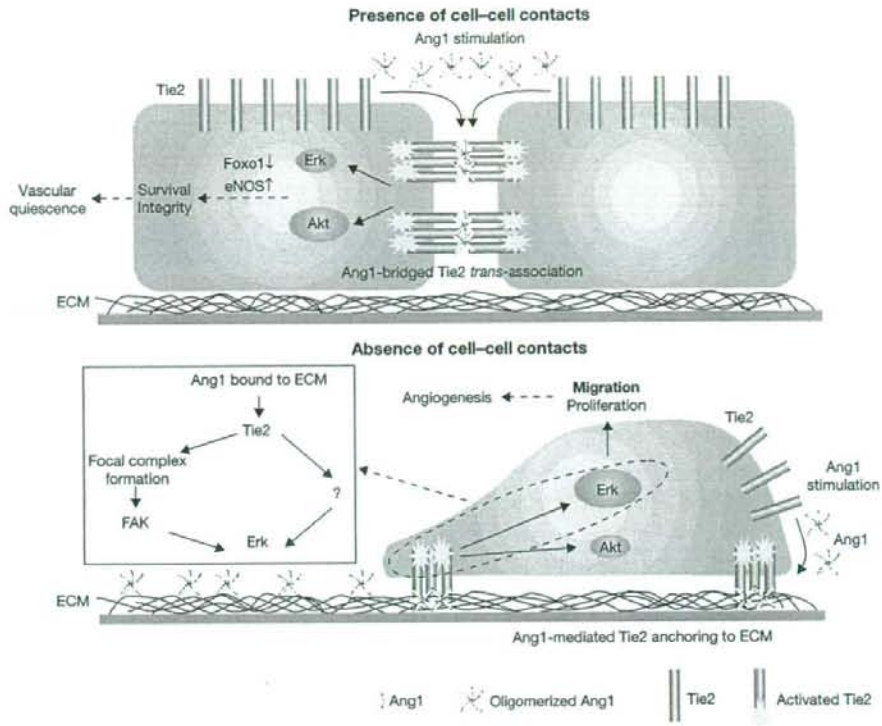

Figure 8 Schematic representation of a proposed model for how Ang1–Tie2 signalling is involved in both vascular quiescence and angiogenesis. (Upper panel) Under confluent conditions, oligomerized Ang1 bridges Tie2 at cell–cell contacts, resulting in formation of *trans*-association of Tie2. *Trans*-associated Tie2 at cell–cell contacts preferentially activates Akt–Foxo1 and Akt–eNOS signalling pathways, which may contribute to maintenance of vascular quiescence by enhancing endothelial survival and integrity (dashed arrows). (Lower panel) In the absence of cell–cell contacts, Tie2 forms a complex with ECM-bound Ang1 at cell–substratum contacts, which is different from focal adhesions, focal complexes and fibrillar adhesion. Ang1–Tie2 anchored to cell–substratum contacts preferentially activates the Erk pathway by inducing FAK-positive focal complex assembly. Ang1, therefore, seems to implicate FAK partly in the activation of Erk. This preferential activation of the Erk pathway induced by Ang1–Tie2 anchored to cell–substratum contacts may contribute to endothelial cell migration and proliferation, thereby promoting angiogenesis (dashed arrows). FC and ECM indicate focal complex and extracellular matrix, respectively.

The presence of cell–cell contacts determines preferential activation of Akt by Ang1 and subsequent phosphorylation of eNOS and Foxo1

Akt phosphorylates the forkhead transcription factor Foxo1 and endothelial nitric oxide synthase (eNOS), which play critical roles in endothelial functions[39,40]. To investigate the biological consequence of preferential activation of Akt by *trans*-associated Tie2, we examined Ang1-induced phosphorylation of Foxo1 and eNOS in the absence and presence of cell–cell contacts. Endothelial cell–cell contacts significantly enhanced COMP–Ang1-induced phosphorylation of Foxo1 and eNOS in HUVECs (Fig. 6a–c). Akt-dependent phosphorylation negatively regulates transcriptional activity of Foxo1 by promoting its nuclear exclusion. Consistently, nuclear export of Foxo1 by COMP–Ang1 was more prominent in confluent HUVECs than in sparse cells (Fig. 6d). Phosphatidylinositol-3 kinase (PI3K) inhibitor, LY294002, and Akt inhibitor impeded COMP–Ang1-induced phosphorylation of Foxo1 and eNOS (Fig. 6e, f). These findings indicate that phosphorylation of Foxo1 and eNOS mediated by PI3K–Akt are preferentially induced by *trans*-associated Tie2 compared to substratum-anchored Tie2.

Distinct gene expression profile in HUVECs upon Ang1 stimulation in the presence or absence of cell–cell contacts

To further clarify the consequence of Tie2 activation at cell–cell contacts and at cell–substratum contacts, we employed DNA microarray analyses. We carried out a global survey of mRNA in either confluent or sparse HUVECs upon COMP–Ang1 stimulation for 1 h. There was a striking difference in the induction of genes between confluent and sparse conditions (Fig. 7a). To confirm the microarray data, expression levels of several genes selectively induced under either sparse or confluent conditions were examined by quantitative real-time PCR analysis. Both basal expression and induction of *Krüppel-like factor (KLF) 10* and *suppressor of cytokine signaling 3 (SOCS3)* were greater in sparse cells than in confluent cells (Fig. 7b, c). In contrast,